The Targeted Delivery of Multicomponent Cargos to Cancer Cells via Nanoporous Particle-Supported Lipid Bilayers

Carlee E. Ashley, Eric C. Carnes, Genevieve K. Phillips, David Padilla, Paul N. Durfee, Page A. Brown, Tracey N. Hanna, Juewen Liu, Brandy Phillips, Mark B. Carter, Nick J. Carroll, Xingmao Jiang, Darren R. Dunphy, Cheryl L. Willman, Dimiter N. Petsev, Deborah G. Evans, Atul N. Parikh, Bryce Chackerian, Walker Wharton, David S. Peabody, & C. Jeffrey Brinker

CONTENTS

Supplementary Figures and Legends

Correspondence and requests for materials should be addressed to C.E.A (ceashle@sandia.gov) or C.J.B. (cjbrink@sandia.gov).

Supplementary Figures and Legends

1. Synthesis and Characterization of Nanoporous Silica Particles and Nanoporous Particle-Supported Lipid Bilayers

The nanoporous silica particles that form the core of the protocell are prepared, as previously described by us[1-2], from a homogenous mixture of water-soluble silica precursor(s) and amphipathic surfactant(s) using either aerosol-assisted evaporation-induced self-assembly (EISA) or solvent extraction-driven self-assembly within water-in-oil emulsion droplets[1] (see Supplementary Methods for more details). Solvent evaporation or extraction concentrates the aerosol or emulsion droplets in surfactant(s), which directs the formation of periodic, ordered structures, around which silica assembles and condenses. Surfactants are removed via thermal calcination, which results in porous nanoparticles with well-defined, uniform pore sizes and topologies. Particles formed via aerosol-assisted EISA ('unimodal' particles) possess an average diameter of approximately 120-nm (after size exclusion-based separation), a Brunauer–Emmer–Teller (BET) surface area in e xcess of 1200 m^2/g, a pore volume fraction of about 50%, and a unimodal pore diameter of 2.5-nm (see Supplementary Fig. 1a – 1c). Particles formed within emulsion droplets ('multimodal' particles) have an average diameter of ~150 nm (after size exclusion-based separation), a BET surface area of > 600 m^2/g, a pore volume fraction of ~65%, and a multimodal pore morphology composed of large (20-30 nm), surface-accessible pores interconnected by 6-12 nm pores (see Supplementary Fig. 1d – 1f). Importantly, the liquid-vapor or liquid-liquid interfacial tensions associated with aerosol or emulsion processing (respectively) enforce a spherical shape with minimal surface roughness. Both types of particles, additionally, have fully accessible three-dimensional pore networks, as evidenced by analysis of nitrogen sorption isotherms.

The high pore volume, surface area, and accessibility of the nanoporous silica cores imparts a high cargo capacity and enables rapid loading of multiple types of therapeutic and diagnostic agents. Unimodal nanoporous cores have a high capacity for low molecular weight chemotherapeutic agents, while multimodal cores possess the large, surface-accessible pores necessary for encapsulation of siRNA, protein toxins, and other high molecular weight cargos (e.g. plasmid DNA). The rate of cargo release can be precisely controlled by the degree to which the silica core is condensed. Incorporating various amounts of AEPTMS, an amine-containing silane, into the sol used to form the nanoporous silica cores reduces the level of achievable condensation and promotes more rapid dissolution of the cores under neutral pH, high ionic strength (i.e. cytosolic) conditions. Particles that contain no AEPTMS dissolve over the course of 2 weeks in a simulated body fluid (data not

shown), while particles that contain 30 mol% AEPTMS dissolve within 24 hours (see Supplementary Fig. 2b). Protocells can, therefore, be adapted for applications requiring continuous or burst release profiles.

Incorporating AEPTMS into the precursor sol used to form nanoporous silica particles accelerates particle dissolution under cytosolic conditions and promotes more rapid release of encapsulated cargo than can be achieved via simple diffusion. AEPTMS-modified particles also have a reduced capacity for weakly basic chemotherapeutic drugs (e.g. doxorubicin), however. Therefore, in order to maximize both capacity and intracellular release, we characterized zeta potential, doxorubicin (DOX) capacity, silica dissolution rates, and DOX release rates as a function of AEPTMS concentration. As we demonstrate in Supplementary Figure 2, unmodified unimodal particles (ζ = -104.5 ± 5.6) have a high capacity for DOX (~1.8 mM per 10^{10} particles) but release only 20% of their encapsulated drug within 24 hours (i.e. the typical doubling time of HCC). Conversely, unimodal particles modified with 30 wt% AEPTMS (ζ = 88.9 ± 5.5) release all of their encapsulated drug within 6 hours but have a reduced DOX capacity (~0.15 mM per 10^{10} particles). Unimodal particles that contain 15 wt% AEPTMS (ζ = -21.3 ± 5.1) retain their high capacity for DOX (~1.1 mM per 10^{10} particles) and release nearly all of their encapsulated drug within 24 hours when exposed to a simulated body fluid; we, therefore, selected these particles for all experiments involving delivery of drugs and drug cocktails (see Figure 6). It is important to note that, while the zeta potential of unimodal silica particles increases as a function of AEPTMS concentration, the pore volume fraction of AEPTMS-modified particles (~45% for particles that contain 30 wt% AEPTMS) is not substantially different from that of unmodified particles (~50%). Therefore, we attribute the decreased DOX capacity of AEPTMS-modified unimodal particles to electrostatic repulsion rather than decreased pore volume. Multimodal particles are included as a control in Supplementary Figure 2 to demonstrate the effect of pore size on DOX capacity and the kinetics of DOX release.

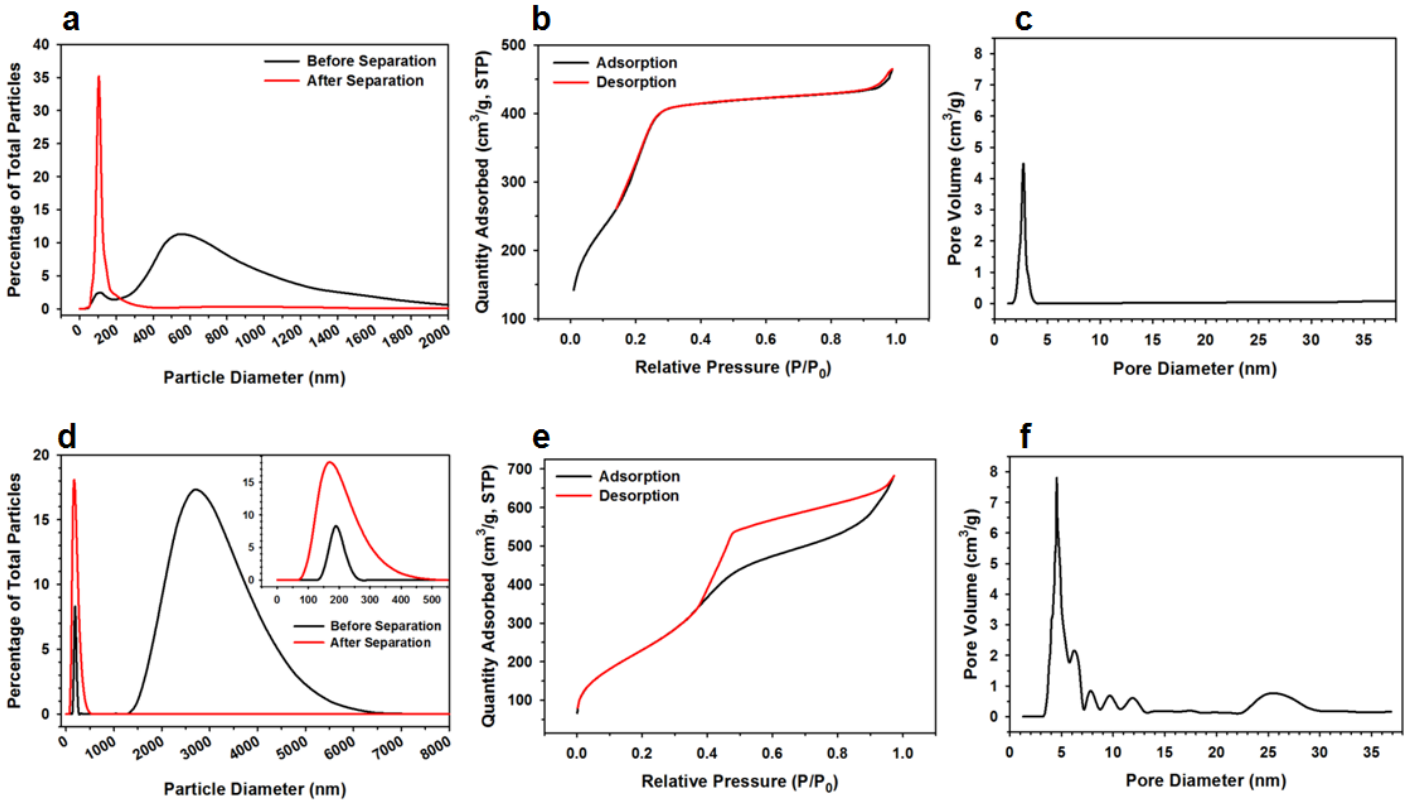

Supplementary Figure 1. Characterization of the nanoporous silica particles that form the protocell core. **(a)** Dynamic light scattering (DLS) of unimodal silica particles, before and after size exclusion-based separation. Particles have an average diameter of ~120 nm after separation. **(b)** Nitrogen sorption isotherm for unimodal particles. The lack of hysteresis indicates that the 3D pore network is fully accessible and that the pores have a uniform size. **(c)** A plot of pore diameter vs. pore volume, calculated from the adsorption isotherm in (b), shows that unimodal particles have a pore size averaging 2.5 nm. **(d)** DLS of multimodal silica particles, before and after size-based separation. Particles have an average particle diameter of ~150 nm after separation. **(e)** Nitrogen sorption isotherm for multimodal particles. The presence of hysteresis is consistent with a network of larger pores interconnected by smaller pores. **(f)** A plot of pore diameter vs. pore volume, calculated from the adsorption isotherm in (e), demonstrates the presence of large (20-30 nm) pores and small (6-12 nm) pores.

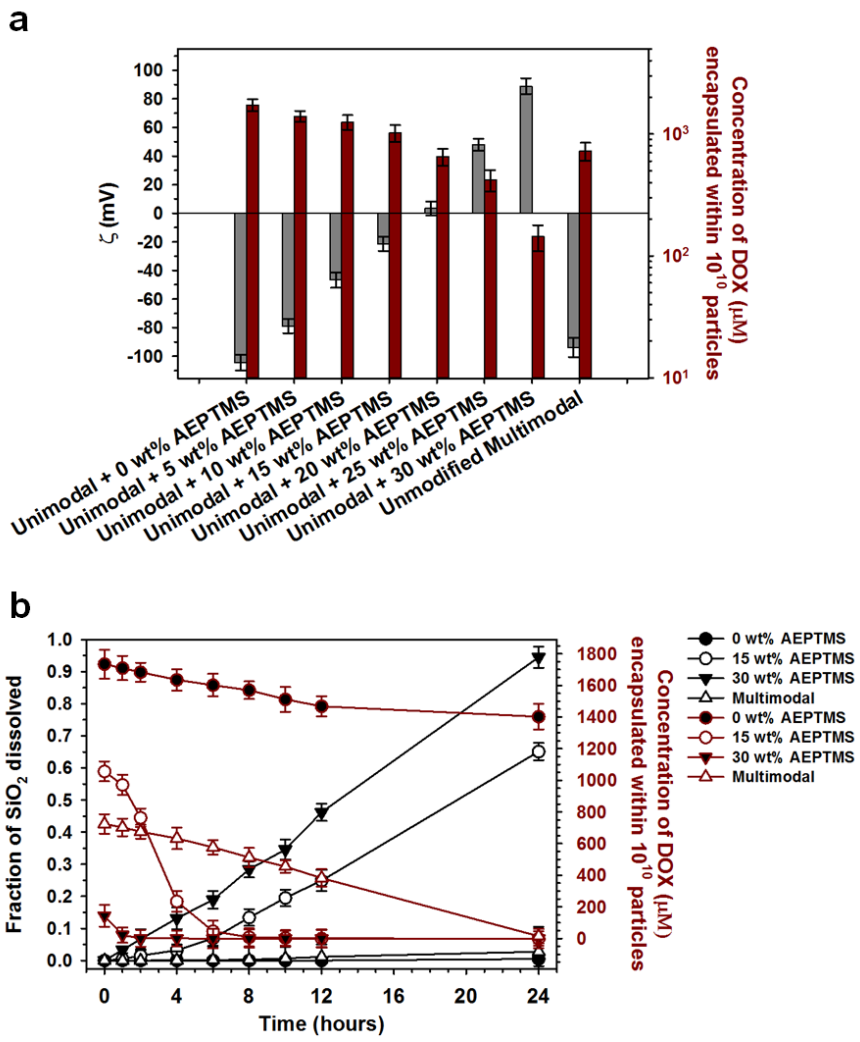

Supplementary Figure 2. The capacities and release profiles of nanoporous silica particles are dependent on pore size and chemistry. **(a)** Zeta potential and doxorubicin (DOX) capacity of unimodal silica particles (~150-nm in diameter) as a function of AEPTMS concentration. Unmodified multimodal silica particles are included as a control. All zeta potential measurements were performed by dispersing particles in a 1 mM KCl buffer at pH 7.0. DOX capacity was determined as described in the Supplementary Methods section. **(b)** The kinetics of silica dissolution and DOX release for unmodified unimodal particles, unimodal particles modified with 15 wt% AEPTMS, unimodal particles modified with 30 wt% AEPTMS, and unmodified multimodal particles when exposed to a simulated body fluid (EMEM with 150 mM NaCl and 10% serum, pH 7.4) at 37°C. The rate of silica dissolution was determined using the molybdenum blue method described by R. K. Iler[3], and the rate of DOX release was determined as described in the Supplementary Methods section. All experiments summarized in this figure were performed using nanoporous silica particles with no supported lipid bilayer. All error bars represent 95% confidence intervals (1.96 σ) for n = 3.

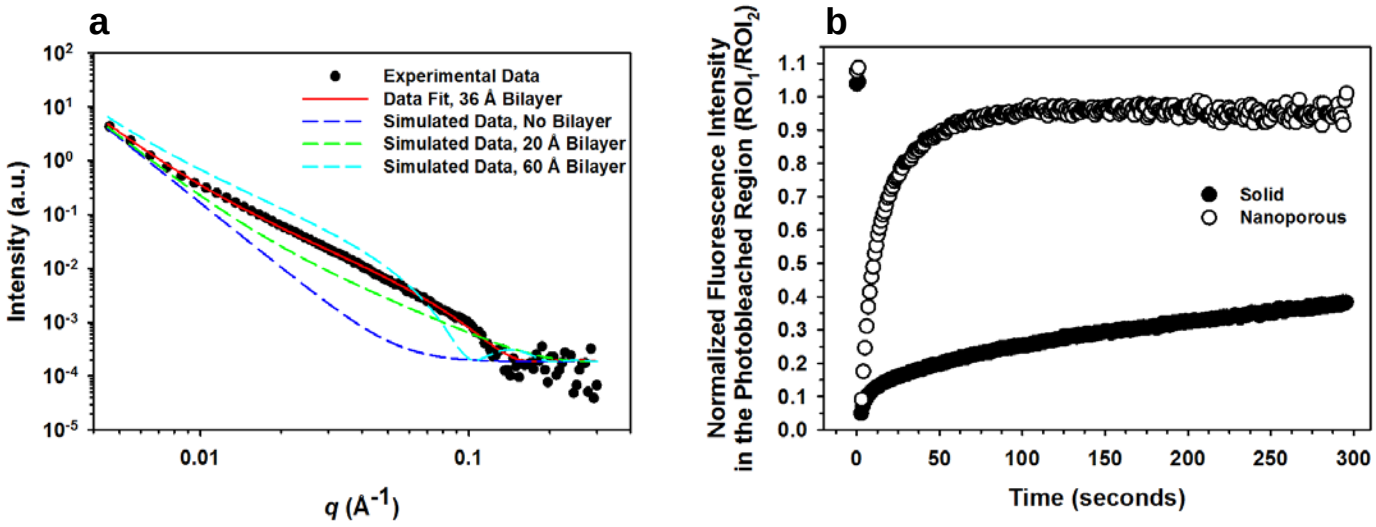

Supplementary Figure 3. Characterization of nanoporous particle-supported lipid bilayers. (a) Small-angle neutron scattering (SANS) data for nanoporous particle-supported DOPC bilayers. The data fit was obtained using a model for polydisperse porous silica spheres with a conformal shell of constant thickness and shows the presence of a 36-Å bilayer at the surface of the silica particles. Simulated SANS data for bilayer thicknesses of 0, 20, and 60 Å are included for comparison. The measured bilayer thickness of 36 Å is consistent with other neutron studies (33-38 Å)[4] performed on planar supported lipid bilayers, and, under these contrast conditions, primarily represents scattering from the hydrogen-rich hydrocarbon core of the lipid bilayer. SANS data were obtained on the LQD beam line at LANSCE (Los Alamos National Laboratories) using a 5% v/v protocell suspension in 100% D_2O PBS buffer. Data were fit using the NCNR SANS data analysis package (NIST). **(b)** Time-dependent fluorescence recovery after photobleaching (FRAP) profiles for DOPC bilayers supported on a 10-µm nanoporous particle or a 10-µm solid (i.e. non-porous) particle. DOPC bilayers were labeled with 5 wt% 18:1-12:0 NBD-PC, and normalized fluorescence intensity was determined as described in the caption to Figure 2b. The low transition temperature of DOPC (T_m = -20°C) prevented us from performing temperature-dependent FRAP experiments to determine the influence of nanoporosity on the melting point of DOPC; as is demonstrated in Fig. 2b, however, we observe a 6°C suppression in the melting point of a DPPC bilayer supported on a nanoporous particle.

Acknowledgement: The SANS experiments summarized in this figure benefited from the use of the Low-Q Diffractometer, LQD, at the Manuel Lujan, Jr. Neutron Scattering Center of the Los Alamos National Laboratory supported by the US. Department of Energy at Los Alamos National Laboratory operated by Los Alamos National Security LLC under contract number DE-AC52-06NA25396.

2. Optimization of the Supported Lipid Bilayer Composition

Protocells are formed via fusion of ~120-nm liposomes to porous silica nanoparticles (100-150 nm in diameter). The resulting supported lipid bilayer (SLB) can be modified with targeting ligands to promote specificity for a given type of cancer and fusogenic peptides to promote endosomal escape of internalized protocells. Although specific affinity is predominantly determined by the fluidity of lipids employed in the SLB and the density of targeting ligands displayed on the SLB, other factors (e.g. overall charge of lipids employed in the SLB and degree of PEGylation of the SLB) can also dramatically influence non-specific interactions between protocells and serum proteins, endothelial cells, etc. Therefore, we optimized the SLB composition in order to maximize colloidal stability, maximize cargo retention, and minimize non-specific interactions with Hep3B, hepatocytes, endothelial cells, and immune cells (PBMCs, B cells, and T cells). We synthesized protocells with SLBs composed of DOPC (zwitterionic, T_m = -20°C), DPPC (zwitterionic, T_m = 41°C), DOTAP (cationic, T_m = -144°C), or DOPG (anionic, T_m = -18°C) with 1 wt% Texas Red®-labeled DHPE; see Supplementary Figure 4 for the structures and transition temperatures of lipids used to optimize the SLB composition. 1 x 10^9 protocells were incubated with 1 x 10^6 Hep3B, hepatocytes, endothelial cells (HUVECs), mononuclear cells (PBMCs), B-lymphocytes, or T-lymphocytes for 1 hour at 4°C. Excess protocells were removed via centrifugation, and the mean fluorescence intensity (MFI) of the resulting cell population was determined via flow cytometry. Total binding was defined as the MFI of cells exposed to protocells modified with 0.500 wt% SP94 (~240 peptides/particle)[5], while non-specific binding was defined as the MFI of cells exposed to unmodified protocells. Specific binding is the difference between total binding and non-specific binding. A high SP94 density (0.500 wt%) was employed to ensure that the specific affinities of protocells with fluid (DOTAP, DOPG, and DOPC) and non-fluid (DPPC) bilayers were approximately equal; bilayer fluidity and peptide density were optimized as described in Figures 4a and 4b.

Lipids with a net positive charge (DOTAP) or net negative charge (DOPG) increase the non-specific binding of protocells to both Hep3B (see Supplementary Fig. 5a) and hepatocytes (see Supplementary Fig. 5b). Employing zwitterionic lipids (DOPC and DPPC) in the SLB minimizes non-specific binding and maximizes specific binding; DPPC protocells have a slightly lower non-specific affinity for Hep3B and hepatocytes than DOPC protocells. Similar results were observed for HUVECs, PBMCs, B cells, and T cells. The total, non-specific, and specific binding of unimodal silica particles (modified with 0.500 wt% SP94 via a heterobifunctional crosslinker reactive toward hydroxyl and sulfhydryl moieties) was included in Supplementary Figures 5a and 5b to demonstrate that nanoporous cores without the presence of a SLB bind

non-specifically to both Hep3B and hepatocytes. Incorporating cholesterol or PEG-2000 PE into the SLB further reduces the non-specific binding of DOPC and DPPC protocells to Hep3B (see Supplementary Fig. 5c). Protocells with SLBs composed of DOPC or DPPC with 30 wt% cholesterol and 5 wt% PEG-2000 remain stable as a colloidal suspension and leak a minimal amount of encapsulated doxorubicin (< 5%) when stored in 0.5X PBS at 4°C for 3 months (data not shown). Furthermore, DOPC and DPPC protocells induce neither oxidative stress nor apoptosis of Hep3B and hepatocytes (data not shown) and are, therefore, attractive alternatives to nanocarriers that employ cationic lipids (e.g. DOTAP, DOTMA, DC-Cholesterol, etc.), which are known to be cytotoxic to many cell types.

To further optimize the specific affinity of DOPC protocells for Hep3B, we modified the SLB with various types of targeting ligands that have an affinity for HCC: the SP94 peptide, which was identified by Lo *et al.* to bind to HCC[6]; diferric transferrin (Tf), a glycoprotein involved in iron transport that binds to a receptor (transferrin receptor, or TfR) upregulated by certain HCC cell lines[7]; a monoclonal antibody against epidermal growth factor receptor (EGFR), which is overexpressed by many types of HCC[8]; and a monoclonal antibody against an unknown HCC surface antigen (CHALV-1). We found that only protocells modified with SP94 retain their affinity for Hep3B at low ligand densities; protocells modified with a low density of Tf, anti-EGFR, or CHALV-1 have K_d values similar to that of the monovalent ligand (data not shown). Furthermore, SP94 has the lowest inherent affinity for hepatocytes, which is likely due to the fact that TfR, EGFR, and the HCC surface antigen targeted by CHALV-1 are not only expressed by HCC but by hepatocytes as well. Given that DOPC protocells modified with a low density of SP94 (0.015 wt%) possess the highest achievable ligand density, the highest affinity for HCC, and the lowest affinity for human hepatocytes, we chose to employ SP94 as the targeting ligand in all of our studies. The above results demonstrate, however, that protocells can be modified with a wide variety of diverse targeting ligands and can, therefore, potentially be adapted to target a variety of cancers and other cells of interest (e.g. pathogenic bacteria or virally-infected mammalian cells).

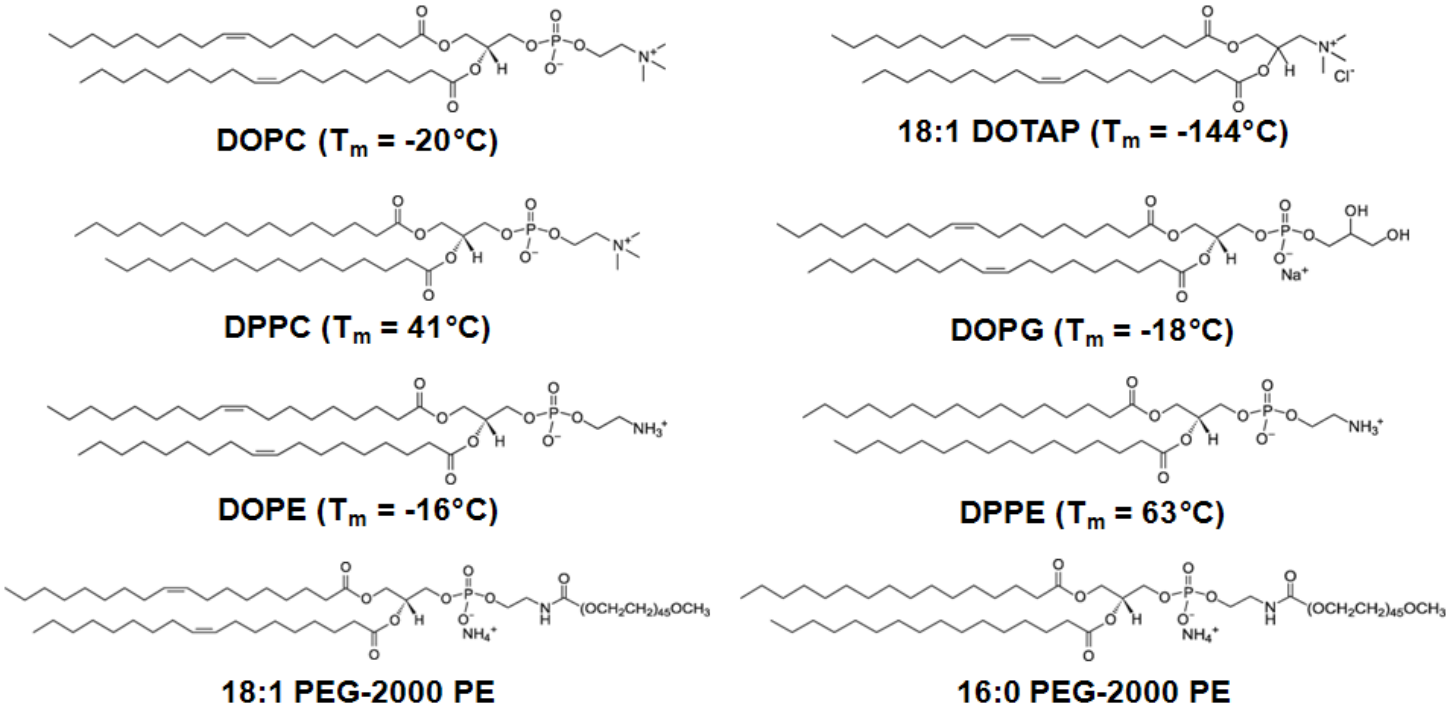

Supplementary Figure 4. Lipids used in SLB optimization studies. Structures and relevant transition temperatures are given for each lipid used to optimize the charge and fluidity of the SLB. DOPE and 18:1 PEG-2000 PE were employed in bilayers composed of fluid lipids (i.e. DOPC, DOTAP, and DOPG), while DPPE and 16:0 PEG-2000 PE were employed in bilayers composed of non-fluid lipids (i.e. DPPC). DOPE and DPPE were included to enable conjugation of the SP94 peptide to the SLB.

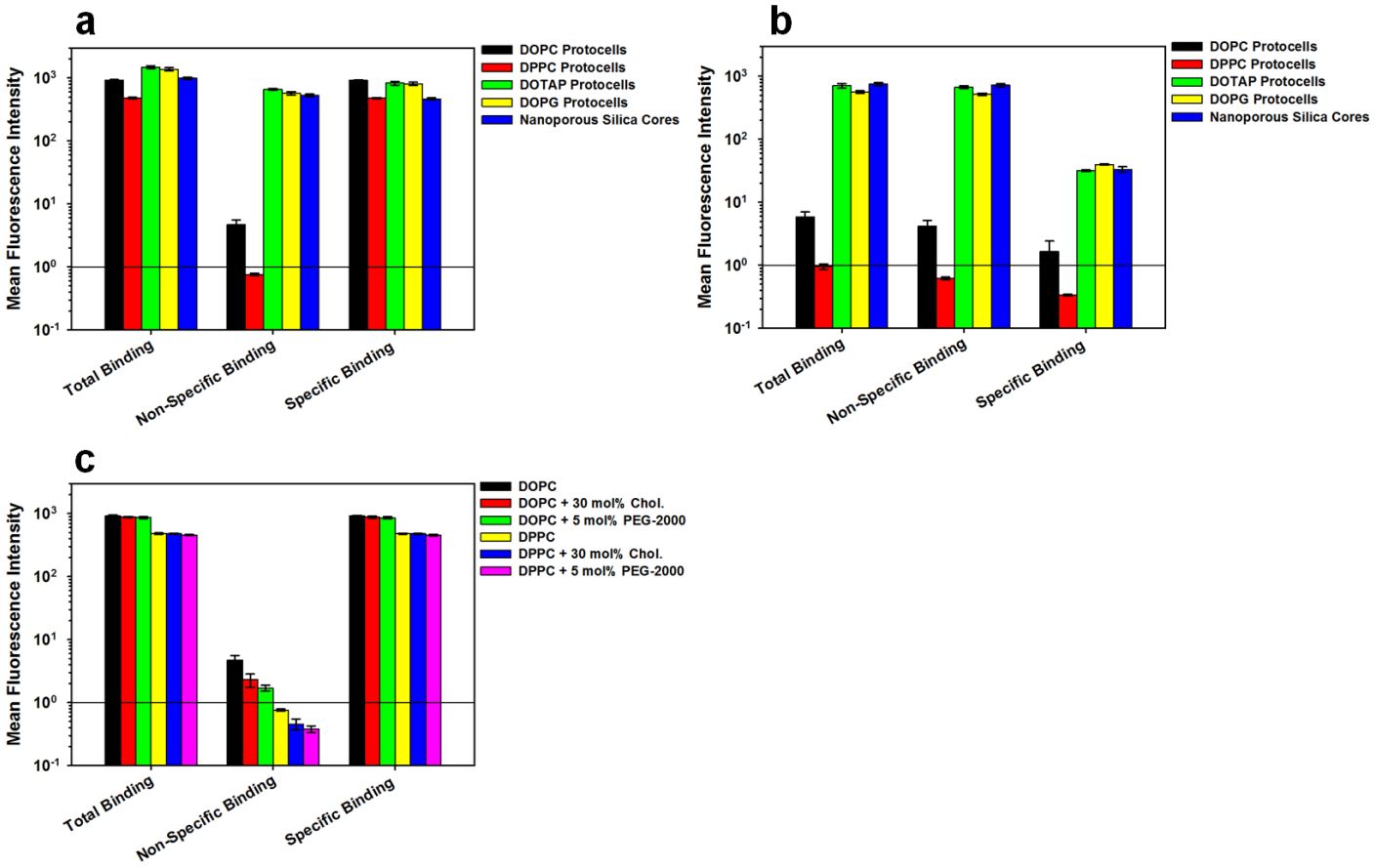

Supplementary Figure 5. Optimization of the SLB composition to minimize non-specific binding of protocells to Hep3B and hepatocytes. The non-specific affinity of protocells modified with 0.500 wt% of the SP94 peptide for Hep3B and hepatocytes is a function of the charge and fluidity of lipids employed in the SLB and the degree to which the SLB is modified with cholesterol or PEG. **(a)** and **(b)** The affinity of SP94-targeted DOPC, DPPC, DOTAP, and DOPG protocells for Hep3B (a) and hepatocytes (b). **(c)** The affinity of SP94-targeted DOPC, DOPC with 30 wt% cholesterol, DOPC with 5 wt% PEG-2000, DPPC, DPPC with 30 wt% cholesterol, and DPPC with 5 wt% PEG-2000 protocells for Hep3B. All error bars represent 95% confidence intervals (1.96 σ) for n = 3.

3. Determination of Dissociation Constants and Additional Surface Binding Data

The SP94 targeting peptide was synthesized with a C-terminal cysteine residue and chemically conjugated to phosphatidylethanolamine (PE) moieties, present in protocell and liposomal bilayers at 1-5 wt%, via a heterobifunctional crosslinker ($SM(PEG)_{24}$) that is reactive toward sulfhydryl and amine moieties and has a 9.5-nm PEG spacer arm. DOPE (T_m = -16°C) was incorporated into DOPC protocells and DOPC liposomes, while DPPE (T_m = 63°C) was incorporated into DPPE protocells, DPPE liposomes, and DSPC liposomes. Excess peptide was removed from targeted protocells and liposomes via centrifugation or dialysis. The average number of peptides displayed on each protocell or liposome was quantified using Tricine SDS-PAGE as described in the Supplementary Methods section; Supplementary Table I lists the standard deviations associated with this method.

To quantify the affinity of SP94-targeted protocells and liposomes (labeled with 1 wt% Texas Red® DHPE) for Hep3B, hepatocytes, endothelial cells (HUVECs), mononuclear cells (PBMCs), B lymphocytes, and T lymphocytes, we incubated various nanocarrier concentrations (from 10 pM to 10 μM, depending on the sample) with 1 x 10^6 cells/mL for 1 hour at 4°C, removed unbound nanocarriers via centrifugation, and characterized the mean fluorescence intensity of the resulting cell population via flow cytometry. We then plotted mean fluorescence intensity versus nanocarrier concentration to generate a saturation binding curve for each sample (see Supplementary Fig. 6 for a sample curve) and used GraphPad Prism (GraphPad Software, Inc.; La Jolla, CA) to calculate dissociation (K_d) constants. K_d values (nM) are inversely related to affinity and represent specific surface binding (except where noted otherwise). See the Supplementary Methods section for more details.

As shown in Supplementary Figure 7, DOPC protocells that display an average of only 6 peptides per particle have a 10^4-fold higher specific affinity for Hep3B than for hepatocytes, HUVECs, PBMCs, B lymphocytes, and T lymphocytes, providing the selectivity necessary for efficacious delivery. Furthermore, the K_d values of DOPC protocells can be precisely modulated from 0.1 nM to 100 nM by simply incorporating increasing amounts of DPPC into the SLB (see Supplementary Figure 8), making protocells adaptable to applications that require nanomolar affinities, such as targeted delivery to blood cancers, as well as applications that require micromolar affinities, such as targeted delivery to tumors when high affinity surface binding can result in reduced penetration.

Supplementary Table I. Errors associated with using Tricine SDS-PAGE to determine the average number of SP94 peptides per protocell or liposome. Standard deviations are given for each peptide density; percent errors are listed in parentheses.

Average Number of SP94 Peptides per Particle	Standard Deviation Associated with Tricine SDS-PAGE Method
6	1 (16.7%)
12	2 (16.7%)
30	4 (13.3%)
60	7 (11.7%)
120	11 (9.17%)
240	17 (7.08%)
512	36 (7.03%)
1024	78 (7.62%)
2048	186 (9.10%)

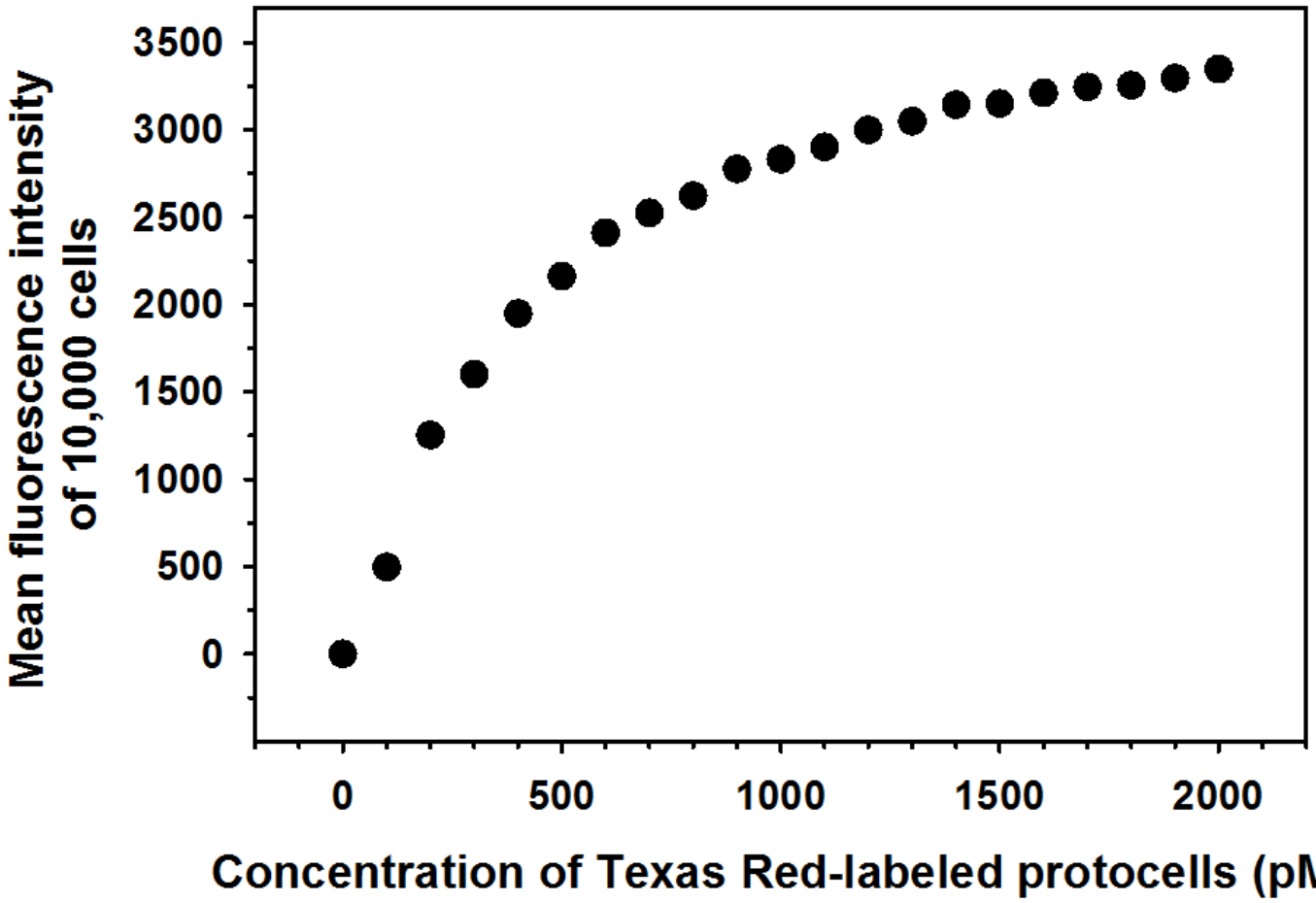

Supplementary Figure 6. Determination of dissociation constants from saturation binding curves. Saturation binding curves were constructed by exposing various concentrations of fluorescently-labeled particles (unmodified and SP94-targeted protocells and liposomes) to a fixed number of cells (HCC and control cells) and measuring the mean fluorescence intensity of each cell population via flow cytometry. The above curve represents the K_d (~0.40 nM) of DOPC protocells modified with 0.060 wt% SP94 (~30 peptides/particle) when exposed to Hep3B.

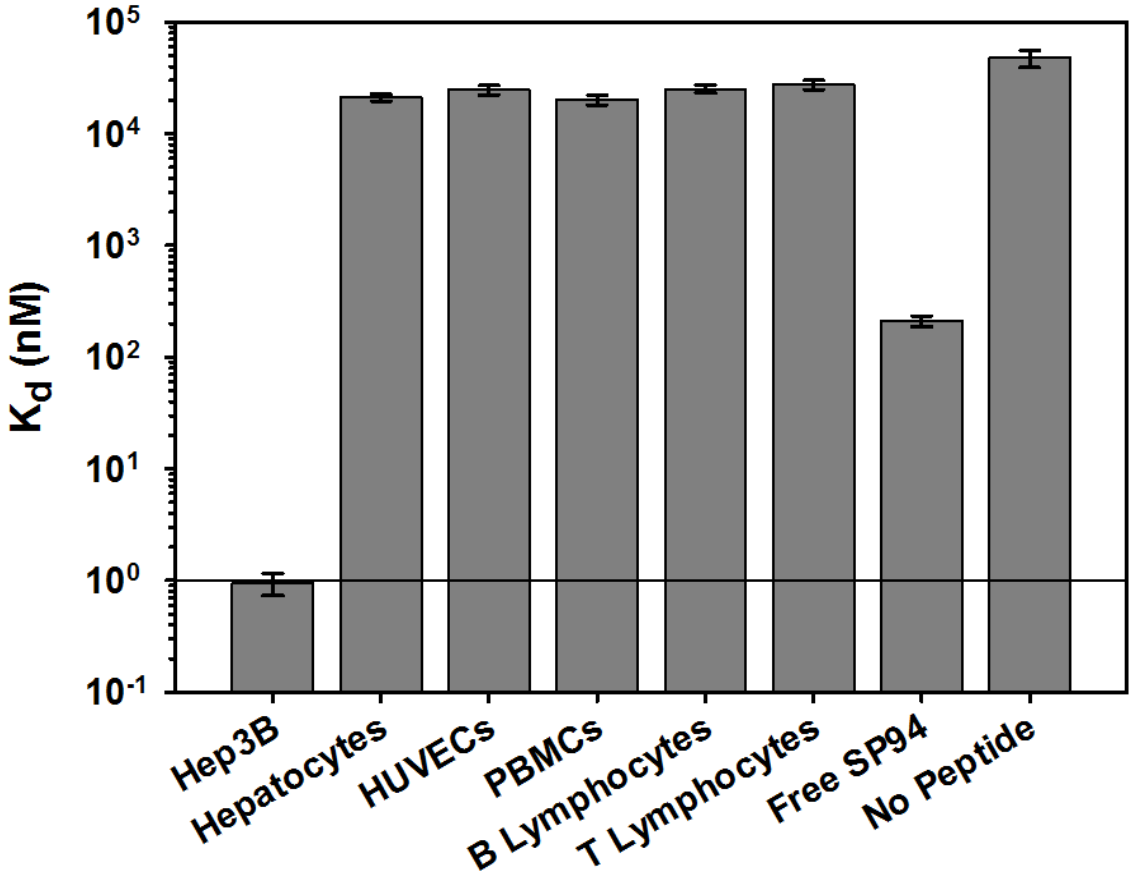

Supplementary Figure 7. SP94-targeted protocells have a high differential affinity for HCC versus hepatocytes and other control cells. K_d values of DOPC protocells modified with 0.015 wt% SP94 (~6 peptides/particle) for Hep3B, human hepatocytes, endothelial cells (human umbilical vein endothelial cells, or HUVECs), peripheral blood mononuclear cells (PBMCs), B-lymphocytes, and T-lymphocytes. The K_d value of free SP94 for Hep3B and the K_d value of unmodified DOPC protocells (no peptide) for Hep3B are included for comparison. All error bars represent 95% confidence intervals (1.96 σ) for n = 5.

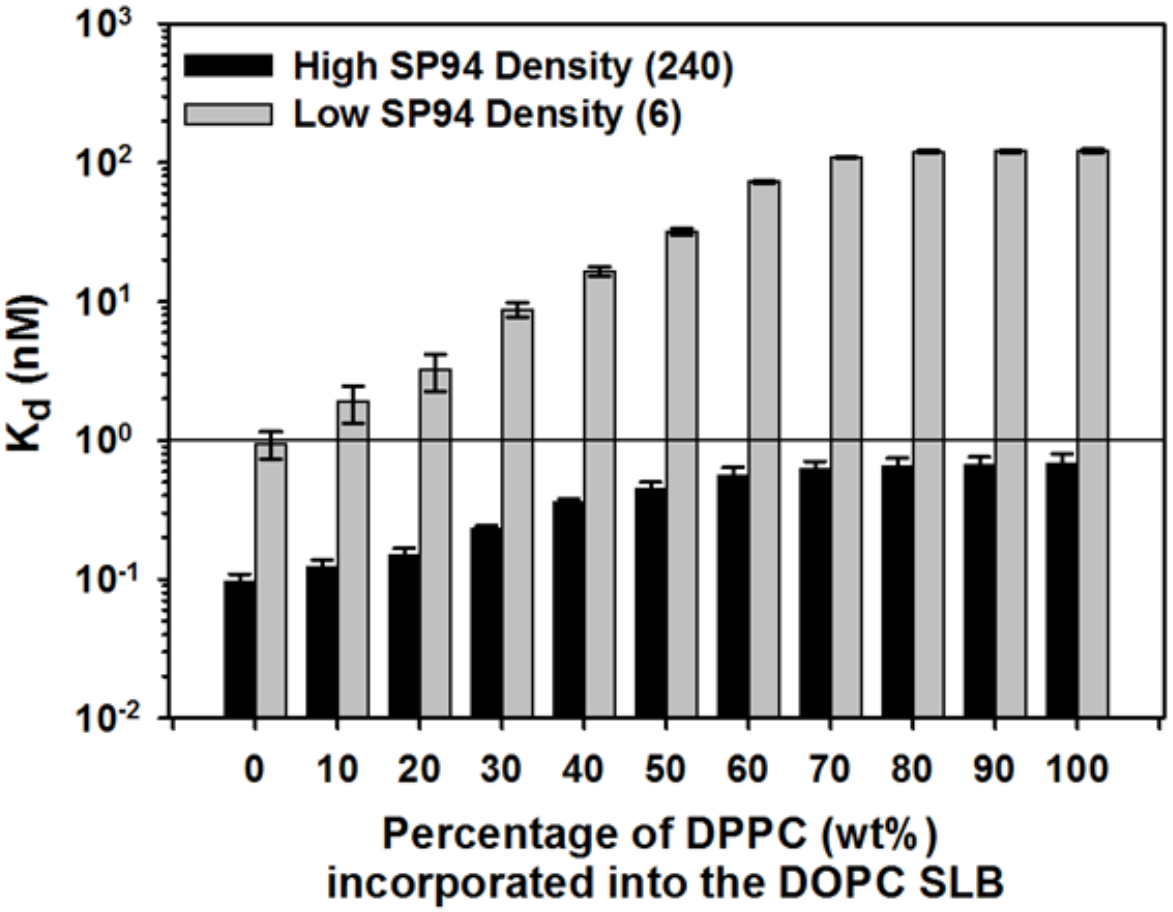

Supplementary Figure 8. The specific affinity of SP94-targeted protocells can be precisely modulated by incorporating various amounts of fluid and non-fluid lipids into the SLB. K_d values of DOPC protocells modified with a high density of SP94 (0.500 wt% or ~240 peptides/particle) remain fairly constant as increasing amounts of DPPC are incorporated into the SLB. Conversely, the K_d values of DOPC protocells modified with a low density of SP94 (0.015 wt% or ~6 peptides/particle) increase with increasing DPPC concentration. All error bars represent 95% confidence intervals (1.96 σ) for n = 5.

4. Selective Internalization of SP94-Targeted Protocells by Hepatocellular Carcinoma

The high differential affinity of SP94-targeted protocells for HCC translates into selective internalization as the experimental temperature is increased from 4°C to 37°C. DOPC protocells that display 0.015 wt% SP94 are rapidly endocytosed by Hep3B ($t_{½}$ = 15 minutes) but not by hepatocytes, as demonstrated by the representative microscopy images shown in Figures 4d and 4e. We have also employed flow cytometry to quantify the average number of SP94-targeted protocells and liposomes that are internalized by Hep3B and hepatocytes (see Supplementary Table II). Furthermore, by labeling DOPE (or DPPE) moieties in the protocell and liposomal bilayers with an amine-reactive form of pHrodo™ (a pH-sensitive red fluorophore, the emission of which increases dramatically at pH ≤ 6.0), we were able to determine the number of particles endocytosed into acidic compartments upon internalization by Hep3B (see the parenthetical values in Supplementary Table II). DOPC protocells modified with a low density of SP94 (0.015 wt%) are internalized by Hep3B more efficiently than corresponding DPPC protocells, DOPC liposomes, or DPPC liposomes, and ~90% of internalized protocells are localized within acidic compartments, which suggests that receptor-mediated endocytosis is the predominant route of internalization. The internalization efficiency of SP94-targeted protocells can be enhanced by optimizing the overall diameter of the nanoporous core. As shown in Supplementary Figure 9, DOPC and DPPC protocells that are ~50-nm in diameter are endocytosed most efficiently by Hep3B. Despite this observation, however, we employ protocells 100-150 nm in diameter for all targeted delivery studies, since cargo capacity scales with the cube of the particle radius: protocells 100-150 nm in diameter have a 25-fold higher capacity for doxorubicin than protocells 50-nm in diameter, whereas protocells 50-nm in diameter are endocytosed by Hep3B only 5-fold more efficiently than protocells 100-150 nm in diameter.

The SP94 peptide directs protocells to lysosomes (versus recycling endosomes) upon endocytosis by HCC, as demonstrated in Supplementary Figure 10. To determine the fate of SP94-targeted protocells upon endocytosis by Hep3B, we exposed 1 x 10^9 DOPC protocells (modified with 30 wt% cholesterol, 5 wt% PEG-2000, 0.015 wt% SP94, and 1 wt% Texas Red®-labeled DHPE) to 1 x 10^6 Hep3B cells for one hour at 37°C. We then employed immunofluorescence to label proteins localized in lysosomes (lysosomal-associated membrane protein-1, or LAMP-1) or recycling endosomes (Rab11a) and used SlideBook software (Intelligent Imaging Innovations, Inc.; Philadelphia, PA) to determine the degree of co-localization between Texas Red®-labeled protocells and either Alexa Fluor® 488-labeled lysosomes or Alexa Fluor® 647-labeled recycling endosomes. We found that there is a positive correlation between protocells and lysosomes but no correlation

between protocells and recycling endosomes (see the Pearson's correlation coefficients in Supplementary Figure 10). We, therefore, modified the protocell SLB with 0.500 wt% of H5WYG, a fusogenic peptide that prevents lysosomal degradation of sensitive cargos (e.g. siRNA and protein toxins), promotes endosomal escape of internalized protocells, and enables cytosolic distribution of protocell-encapsulated cargos (see Supplementary Fig. 11b). Internalization of protocells into acidic compartments plays two critical roles in the targeted delivery of encapsulated cargo(s) to HCC: acidic conditions (1) 'activate' the histidine-rich fusogenic peptide, which becomes protonated at pH < 6.0 and destabilizes endosomal membranes via the 'proton-sponge' mechanism[9] and (2) destabilize the protocell SLB (see Supplementary Figure 12), thereby allowing encapsulated cargo to diffuse out of the nanoporous core (see Fig. 6c). Endosomal escape of internalized protocells combined with destabilization of the protocell's SLB allow cargos encapsulated within SP94-targeted protocells to become concentrated in the cytosol of HCC cells.

Supplementary Table II. The average number of SP94-targeted protocells and liposomes internalized by Hep3B and hepatocytes. Average numbers of DOPC protocells, DPPC protocells, DOPC liposomes, and DPPC liposomes (all 100-150 nm in diameter and modified with 30 wt% cholesterol, 5 wt% PEG-2000, and 0.015 wt% SP94) that are internalized by Hep3B and hepatocytes within one hour at 37°C. Values listed in the second and third columns refer to the average number of *total* particles that are internalized by a single Hep3B or hepatocyte cell; values listed in parentheses refer to the average number of particles internalized into acidic compartments. Average numbers of non-targeted protocells that are internalized by Hep3B and hepatocytes within one hour at 37°C are included for comparison; similar values were observed for non-targeted DOPC and DPPC liposomes.

Type of Particle	**Average Number of Particles Internalized per Hep3B Cell**	**Average Number of Particles Internalized per Hepatocyte**
SP94-Targeted DOPC Protocells	543 ± 21 (498 ± 19)	9 ± 4
Non-targeted DOPC Protocells	6 ± 4	5 ± 1
SP94-Targeted DPPC Protocells	122 ± 13 (107 ± 16)	4 ± 2
Non-targeted DPPC Protocells	2 ± 2	4 ± 1
SP94-Targeted DOPC Liposomes	131 ± 27 (98 ± 17)	13 ± 8
SP94-Targeted DPPC Liposomes	103 ± 15 (94 ± 8)	5 ± 3

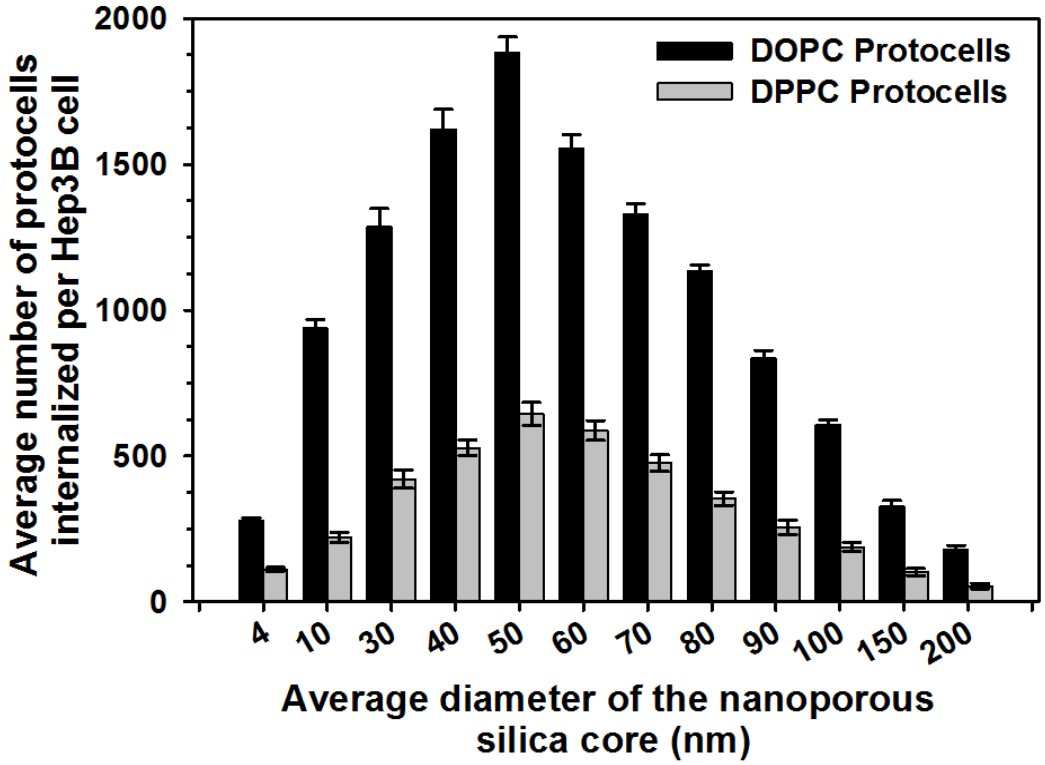

Supplementary Figure 9. The internalization efficacy of SP94-targeted protocells is dependent on the size of the nanoporous core. As the diameter of the nanoporous core increases, fewer SP94-targeted DOPC and DPPC protocells are endocytosed by each Hep3B cell, which is, presumably, due to the observation that membrane wrapping occurs most effectively for 30- to 60-nm particles[10]. Protocells were modified with 30 wt% cholesterol, 5 wt% PEG-2000, and 0.015 wt% SP94 and incubated with 1 x 10^6 Hep3B cells for 1 hour at 37°C. Error bars represent 95% confidence intervals (1.96 σ) for n = 3.

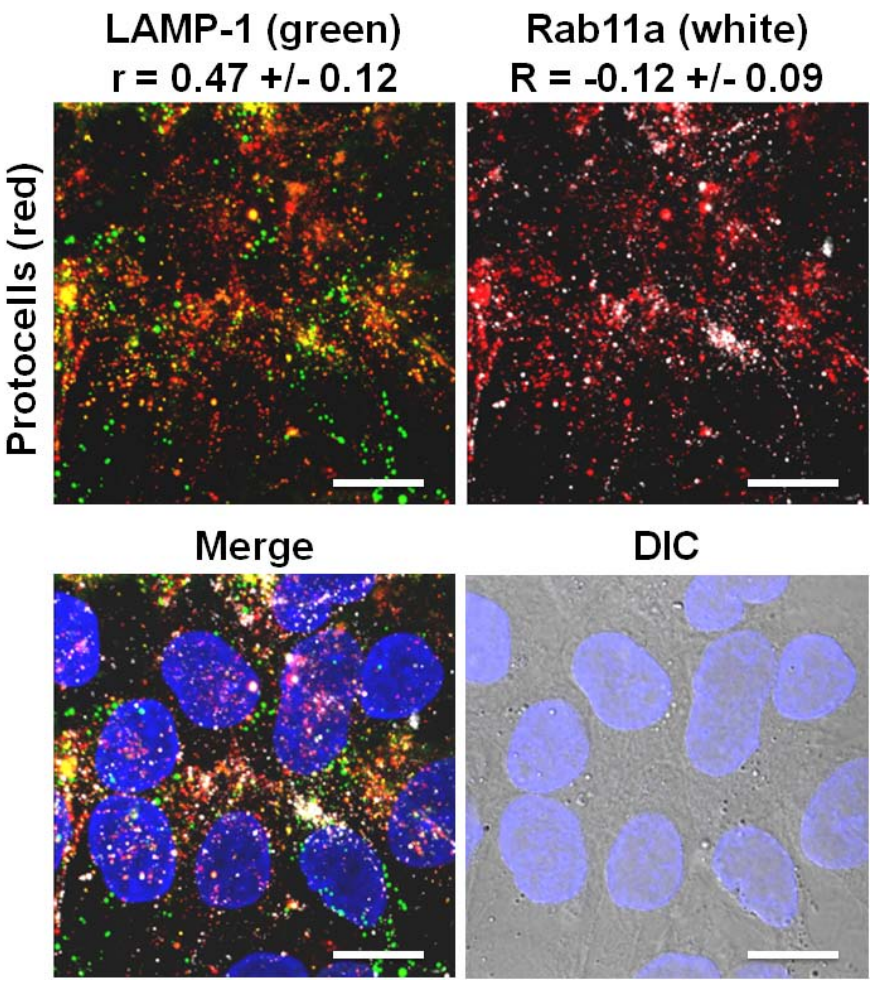

Supplementary Figure 10. The SP94 peptide directs protocells to lysosomes upon endocytosis by HCC. As evidenced by the positive Pearson's correlation (r) between protocells (labeled with 1 wt% Texas Red®-labeled DHPE) and LAMP-1 (labeled with Alexa Fluor® 488), SP94-targeted DOPC protocells are primarily directed to lysosomes upon endocytosis by Hep3B. Conversely, the Pearson's correlation between protocells and Rab11a (labeled with Alexa Fluor® 647) is≈ 0, which indicates that protocells are not typically localized within $Rab11a^+$ recycling endosomes. Differential Interference Contrast (DIC) images were employed to define the boundaries of Hep3B cells, the nuclei of which are labeled with DAPI, such that pixels outside of the cell boundaries could be disregarded when calculating Pearson's correlation coefficients (expressed as the mean value ± the standard deviation for n = 3 x 50 cells). Scale bars = 10 μm.

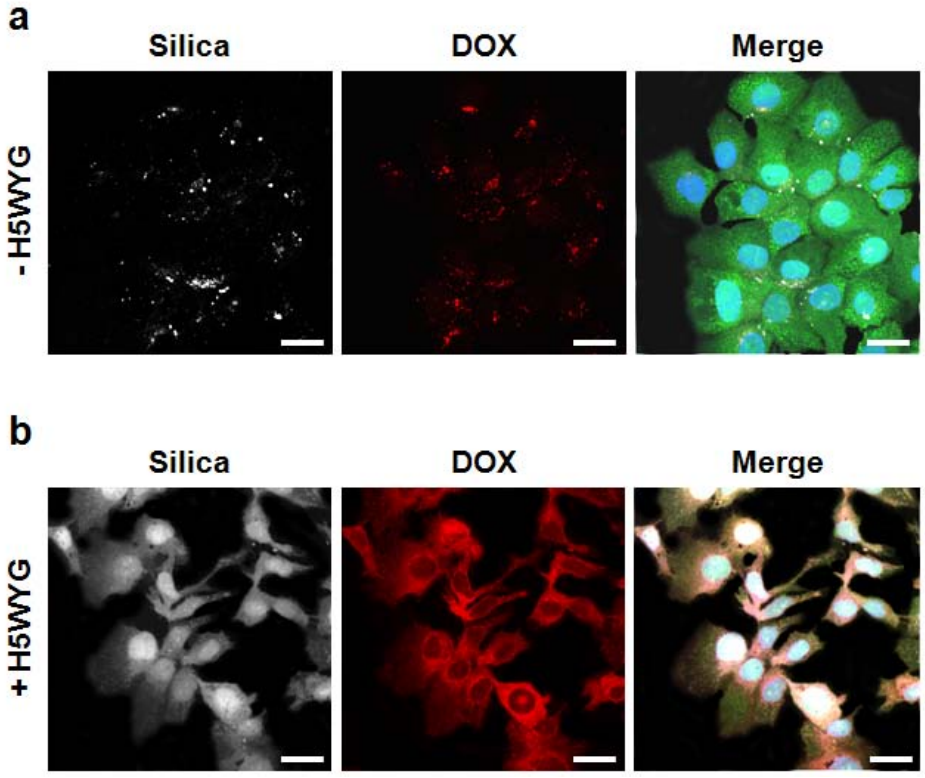

Supplementary Figure 11. The H5WYG fusogenic peptide is necessary to promote endosomal escape of SP94-targeted protocells and cytosolic distribution of protocell-encapsulated cargos. **(a)** Confocal fluorescence microscopy image of Hep3B cells that were exposed to DOPC protocells, modified with 0.015 wt% SP94, for 12 hours at 37°C. **(b)** Confocal fluorescence microscopy image of Hep3B cells that were exposed to DOPC protocells, modified with 0.015 wt% SP94 and 0.500 wt% H5WYG, for 12 hours at 37°C. Protocells are loaded with doxorubicin (red), and their nanoporous cores are labeled with Alexa Fluor® 647 (white). Hep3B cells are stained with CellTracker™ Green CMFDA and DAPI; the high cytosolic concentration of DOX in (b) is likely responsible for cell shrinkage and other changes in normal cellular morphology. Scale bars = 20 μm.

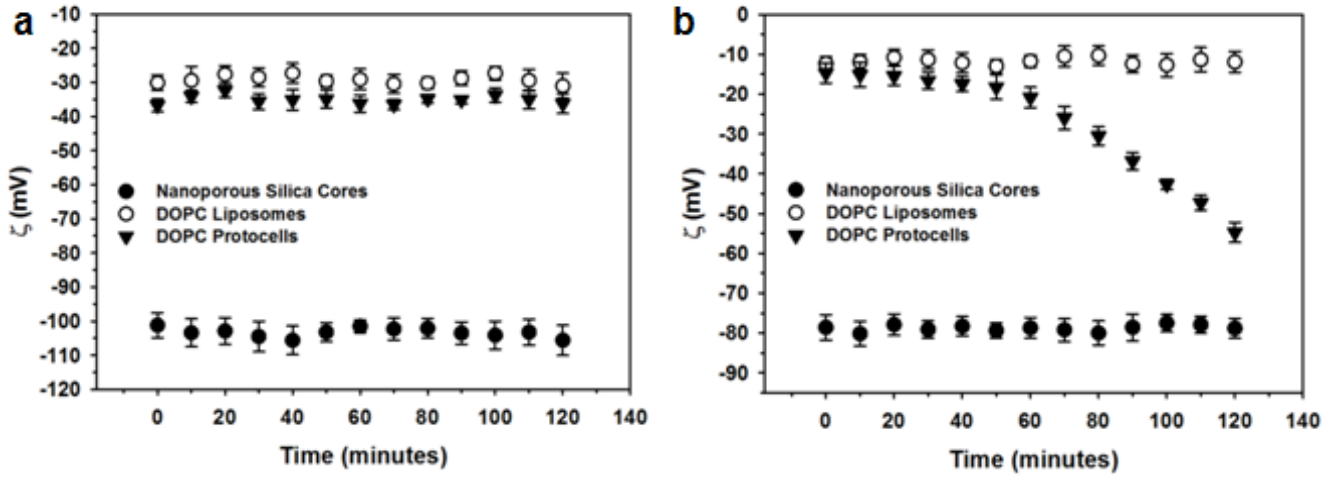

Supplementary Figure 12. Zeta potential measurements of DOPC protocells reveal that acidic conditions destabilize the SLB. Zeta potential (ζ) values of DOPC liposomes, DOPC protocells, and nanoporous silica cores when exposed to 1 mM KCl at pH 7 **(a)** or 1 mM KCl at pH 5 **(b)** for 2 hours at 37°C. Acidic conditions destabilize the SLB, as evidenced by the time-dependent decrease in the zeta potential of DOPC protocells when exposed to the pH 5 buffer. Zeta potential values of DOPC liposomes and silica nanoparticles at pH 7 and pH 5 correlate well with those that have been reported previously[11]. All error bars represent 95% confidence intervals (1.96 σ) for n = 3.

5. Delivery of siRNA Cocktails via SP94-Targeted Protocells

RNA interference (RNAi) has been widely used to suppress expression of various proteins necessary for cancer cell proliferation and survivability via sequence-specific, post-transcriptional gene silencing that is typically mediated by siRNA or microRNA (miRNA)[12-13]. siRNAs (~21-base-pair segments of double-stranded RNA) are attractive as anti-cancer agents given their ability to promote RNAi in mammalian cells without eliciting an interferon response[14]. Furthermore, Davis, *et al.* recently demonstrated that siRNA, upon systemic administration via transferrin-targeted polymeric nanoparticles can effectively inhibit specific genes in humans with solid tumors[15]. Thus, targeted delivery of siRNA shows great promise in effectively treating a variety of cancers[16].

A plethora of reagents that employ cationic lipids (e.g. Lipofectamine^{TM}) or polymers (e.g. polycationic peptides, polyethyleneimine, etc.) to electrostatically complex, condense, and deliver plasmid DNA, antisense oligonucleotides, miRNA, siRNA, etc. are commercially available but result in non-specific transfection of most eukaryotic cell types. Furthermore, cationic lipid-nucleic acid complexes (so-called 'lipoplexes') are known to be cytotoxic, and their transfection efficiency and colloidal stability tend to be limited in the presence of serum and certain salts[17]. Conversely, zwitterionic lipids are incapable of efficiently compacting nucleic acids, even in the presence of divalent cations[18]. Thus, protocells offer yet another advantage over liposomes since our multimodal silica nanoparticles can be rapidly loaded with siRNA and other types of nucleic acids by simply soaking AEPTMES-modified nanoparticles in a solution of the desired cargo(s). Furthermore, fusion of DOPC liposomes to siRNA-loaded cores results in the formation of a zwitterionic SLB that, as described above, reduces non-specific binding, improves colloidal stability, and mitigates the cytotoxicity associated with cationic liposomes and lipoplexes.

The abnormal activation of certain growth factor receptors, including epidermal growth factor receptor (EGFR), vascular endothelial growth factor receptor-2 (VEGFR-2), and platelet-derived growth factor receptor-α (PDGFR-α) has been implicated in hepatocarcinogenesis[19], and siRNA-mediated silencing of EGFR has been demonstrated to enhance the susceptibility of various cancer types to chemotherapeutic drugs and to induce growth arrest and apoptosis of tumor cells *in vitro* and *in vivo*[20]. To this end, we loaded AEPTMS-modified multimodal silica nanoparticles ($\zeta = 24 \pm 3.4$ mV) with a siRNA cocktail that induces sequence-specific degradation of EGFR, VEGFR-2, and PDGFR-α messenger RNA (mRNA) by soaking nanoporous cores (25 mg/mL) in a 100 μM solution of the siRNA cocktail for 2 hours at 4°C. Unencapsulated cargo was removed via

centrifugation, DOPC liposomes containing 5 wt% DOPE, 30 wt% cholesterol, and 5 wt% PEG-2000 were immediately fused to siRNA-loaded cores, and the SLB was modified with 0.015 wt% of the SP94 peptide and 0.500 wt% of the H5WYG peptide. DOPC liposomes were loaded with siRNA[21] for comparative purposes but were not employed as a control in the majority of experiments described below due to inefficient loading: 10^{10} DOPC protocells can encapsulate ~10 μM of siRNA (95.6% of which is released upon exposure to a pH 5.0 buffer for 24 hours), while 10^{10} DOPC liposomes only complex ~8 nM of siRNA.

Upon exposure to Hep3B (1 x 10^6 cells/mL), SP94-targeted DOPC protocells loaded with the siRNA cocktail induce a dose-dependent (see Supplementary Fig. 13a) and time-dependent (see Supplementary Fig. 13b) decrease in expression of EGFR, VEGFR-2, and PDGFR-α. The concentrations of protocell-delivered siRNA necessary to silence 50% of EGFR, VEGFR-2, and PDGFR-α expression (IC_{50}) within 24 hours are 6.68 nM, 4.18 nM, and 12.8 nM, respectively. Furthermore, protocells loaded with the siRNA cocktail (10 nM total concentration) decrease EGFR, VEGFR-2, and PDGFR-α expression in Hep3B by > 90% within 72 hours (see Supplementary Fig. 13b, 13c, and 13d) without affecting protein levels in hepatocytes (see Supplementary Fig. 13c and 13e). Due to the high specific affinity of SP94-targeted protocells for HCC combined with the enhanced capacity conferred by the multimodal nanoporous core, DOPC protocells loaded with 10 nM of the siRNA cocktail kill 50% of Hep3B within 36 hours without affecting the viability of hepatocytes (see Supplementary Figure 14). In contrast, DOPC liposomes loaded with 10 nM of the siRNA cocktail kill only 8% of Hep3B upon continual exposure for 72 hours.

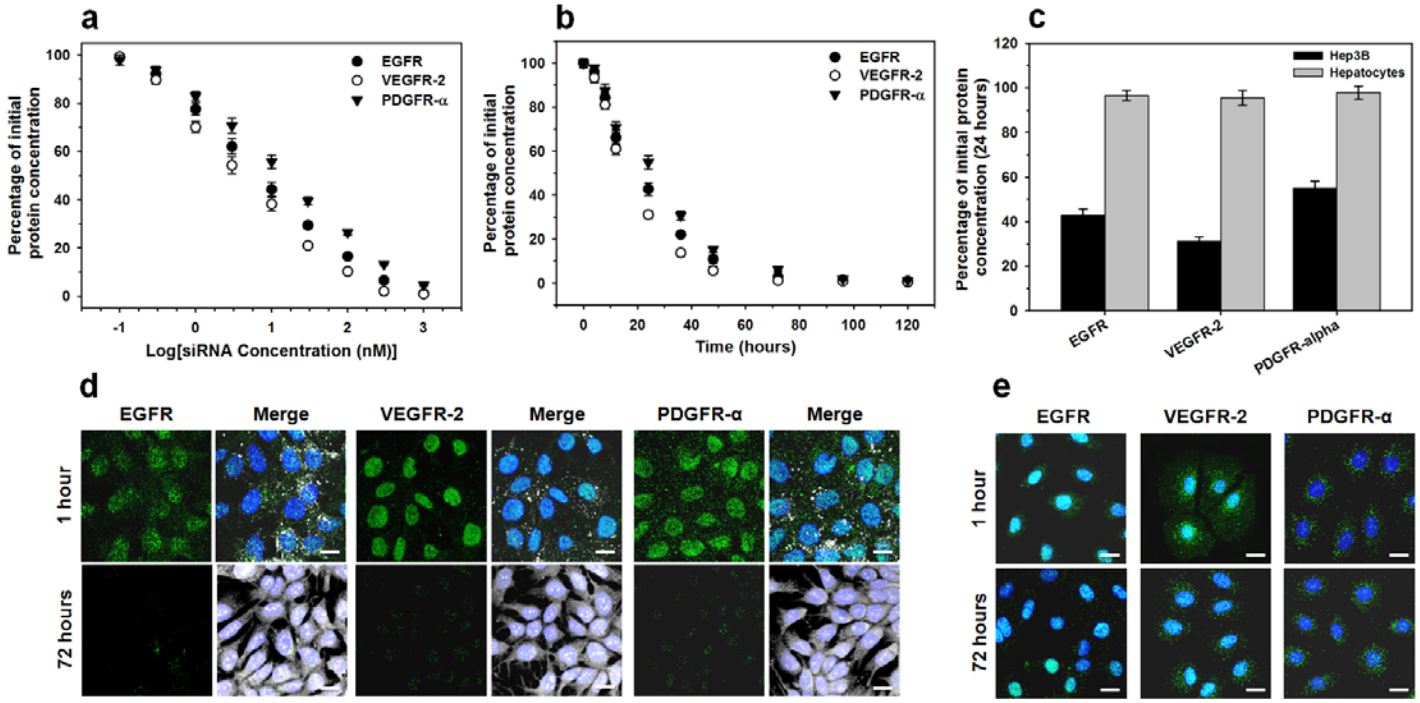

Supplementary Figure 13. SP94-targeted DOPC protocells loaded with a siRNA cocktail silence expression of target proteins in HCC but not hepatocytes. (a) and **(b)** SP94-targeted protocells loaded with a siRNA cocktail that silences expression of EGFR, VEGFR-2, and PDGFR-α induce a dose- (a) and time-dependent (b) decrease in target protein concentrations (determined via immunofluorescence) when exposed to Hep3B. **(c)** SP94-targeted protocells loaded with 10 nM of the siRNA cocktail reduce EGFR, VEGFR-2, and PDGFR-α expression in Hep3B but not hepatocytes. Error bars in (a) – (c) represent 95% confidence intervals (1.96 σ) for n = 3. **(d)** and **(e)** Confocal fluorescence microscopy was utilized to confirm that SP94-targeted protocells are exclusively endocytosed by Hep3B (d) and, therefore, do not induce a decrease in EGFR, VEGFR-2, or PDGFR-α concentrations when exposed to hepatocytes (e). Upon endocytosis by Hep3B, SP94-targeted DOPC protocells with Alexa Fluor® 647-labeled nanoporous cores (white) are initially (1 hour) localized within endosomes but become dispersed in the cytosol within 4 hours; over the course of 72 hours, siRNA molecules are released from the nanoporous core and silence nearly all EGFR, VEGFR-2, and PDGFR-α (green) expression. Nuclei are stained with DAPI. Scale bars in (d) and (e) = 20 μm.

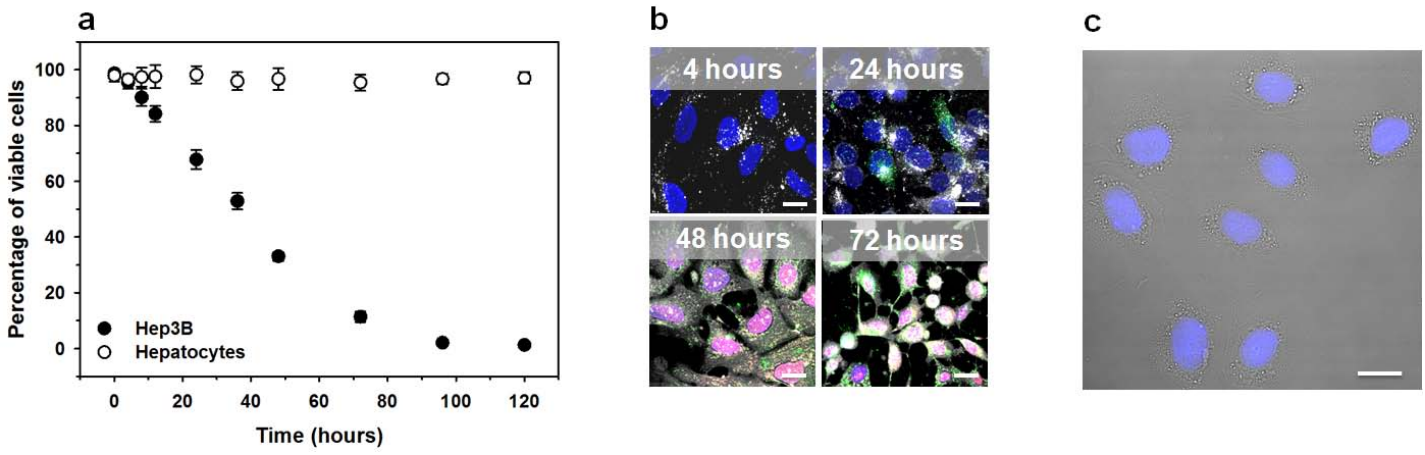

Supplementary Figure 14. SP94-targeted DOPC protocells loaded with a siRNA cocktail induce apoptosis of HCC within 24 hours. (a) Time-dependent viability of Hep3B and hepatocytes exposed to SP94-targeted DOPC protocells loaded with the siRNA cocktail (10 nM total concentration). Alexa Fluor® 488-labeled annexin V and propidium iodide were use to distinguish viable (double-negative) from non-viable (single- or double-positive) cells. Error bars represent 95% confidence intervals (1.96 σ) for n = 3. **(b)** Upon exposure to siRNA-loaded protocells, Hep3B cells become positive for Alexa Fluor® 488-labeled annexin V (green) within 24 hours and double-positive for annexin V (green) and propidium iodide (red) within 48 hours. **(c)** As evidenced by the DIC image, hepatocytes remain double-negative for annexin V and propidium iodide when exposed to SP94-targeted, siRNA-loaded protocells for 1 week. Nuclei are stained with DAPI. Scale bars in (b) and (c) = 20 μm.

6. Delivery of Protein Toxins via SP94-Targeted Protocells

Due to the presence of large (20-30 nm), surface-accessible pores, multimodal silica nanoparticles can be readily loaded with various protein toxins, including diphtheria, cholera, and ricin toxins. Furthermore, the high degree of differential specificity exhibited by DOPC protocells modified with a low density of targeting ligands enables selective delivery of especially cytotoxic agents (e.g. ricin toxin) to cancer. Diphtheria toxin is an exotoxin secreted by *Corynebacterium diphtheriae* that is composed of two subunits (A and B) held together by a disulfide bond. The B-chain (39 kDa) facilitates receptor-mediated endocytosis of the toxin, while the A-chain (24 kDa) inhibits protein synthesis in eukaryotic host cells by using NAD as a substrate to catalyze the ADP-ribosylation of aminoacyl-transferase II (EF-2)[22]. Catalytically-active A-chain can be generated by exposing the native toxin to trypsin and a reducing agent (e.g. dithiothreitol) and has been employed in tumor-specific immunotoxins to inhibit the growth of cancer cells *in vitro* and *in vivo*[5]. We have, therefore, loaded AEPTMS-modified multimodal silica nanoparticles ($\zeta = 24 \pm 3.4$ mV) with diphtheria toxin A-chain (DTA) by soaking nanoporous cores (25 mg/mL) in a 100 μM solution of purified DTA[23] for 2 hours at 4°C. Unencapsulated cargo was removed via centrifugation, and DOPC liposomes containing 5 wt% DOPE, 30 wt% cholesterol, and 5 wt% PEG-2000 were immediately fused to DTA-loaded cores. The resulting SLB was modified with 0.015 wt% of the SP94 peptide and 0.500 wt% of the H5WYG peptide; excess peptide was removed via centrifugation. DOPC liposomes were loaded with DTA [24] for comparative purposes but were not employed as a control in the majority of experiments described below due to the low achievable loading efficiency: 10^{10} DOPC protocells can encapsulate ~2 μM of DTA (89.7% of which is released upon exposure to a pH 5.0 buffer for 24 hours), while 10^{10} DOPC liposomes can only encapsulate ~1 nM of DTA.

Upon exposure to Hep3B (1×10^6 cells/mL), SP94-targeted DOPC protocells loaded with DTA cause a dose-dependent (see Supplementary Fig. 15a) and time-dependent (see Supplementary Fig. 15b) decrease in nascent protein synthesis. The IC_{50} value of DTA-loaded protocells is 92.0 nM; protocells that encapsulate 100 nM of DTA cause a 50% reduction in nascent protein synthesis within 24 hours and a 90% reduction within 72 hours. SP94-targeted protocells loaded with DTA induce caspase-8/3-dependent apoptosis in 50% of Hep3B cells within ~18 hours at concentrations < 100 nM but have no cytotoxic effect on hepatocytes (see Supplementary Figure 16). In contrast, DOPC liposomes loaded with 100 nM of DTA induce apoptosis in < 1% of Hep3B, even when exposed continually for 2 weeks.

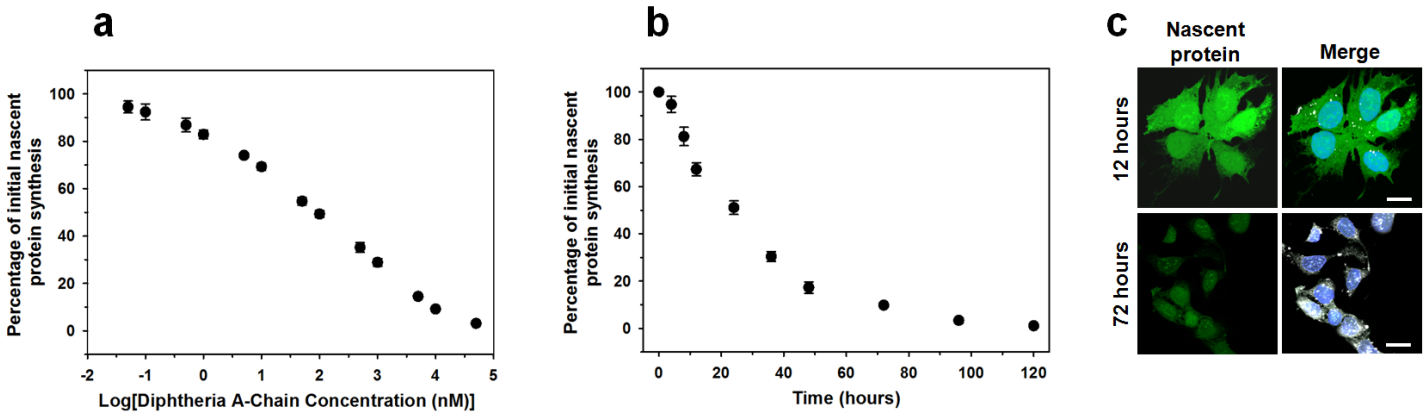

Supplementary Figure 15. SP94-targeted DOPC protocells loaded with diphtheria toxin A-chain cause a reduction in nascent protein synthesis upon endocytosis by HCC. **(a)** and **(b)** SP94-targeted protocells loaded with DTA cause a dose-dependent (a) and time-dependent (b) decrease in nascent protein synthesis when exposed to Hep3B. Error bars represent 95% confidence intervals (1.96 σ) for n = 3. **(c)** A confocal fluorescence microscopy image that confirms the result shown in (b). Nascent protein synthesis was quantified using an Alexa Fluor® 488-labeled derivative of methionine (green), and protocell endocytosis was tracked using Alexa Fluor® 647-labeled nanoporous cores (white). Hep3B nuclei are stained with DAPI. Scale bars = 20 μm.

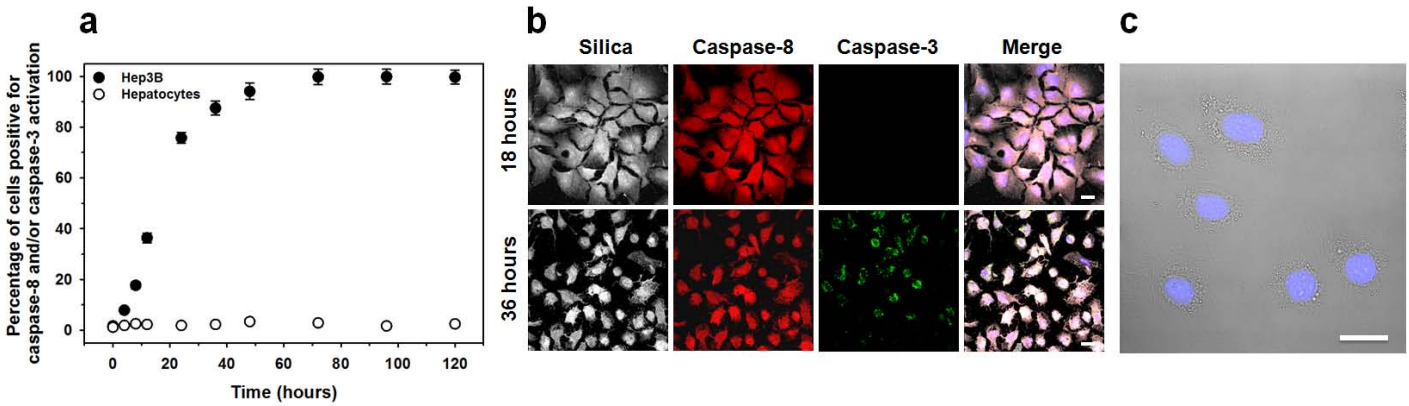

Supplementary Figure 16. SP94-targeted DOPC protocells loaded with diphtheria toxin A-chain induce apoptosis of HCC but not hepatocytes. **(a)** Percentage of Hep3B and hepatocytes positive for caspase-8 and/or caspase-3 activation upon incubation with SP94-targeted DOPC protocells loaded with 100 nM of DTA for various periods of time at 37°C. Error bars represent 95% confidence intervals (1.96 σ) for n = 3. **(b)** DTA-loaded protocells with Alexa Fluor® 647-labeled cores (white) induce caspase-8 activation (red) within 18 hours and capase-3 activation (green) within 36 hours when exposed to Hep3B. **(c)** As evidenced by the DIC image, SP94-targeted protocells loaded with DTA induce neither caspase-8 nor caspase-3 activation when exposed to hepatocytes for > 1 week. Nuclei are stained with DAPI in all fluorescence images. Scale bars in (b) and (c) = 20 μm.

Supplementary Materials and Methods

1. Materials

General Reagents

Absolute ethanol, hydrochloric acid (37%), tetraethyl orthosilicate (TEOS, 98%), 3-aminopropyltriethoxysilane (APTES, ≥ 98%), 3-[2-(2-aminoethylamino)ethylamino]propyltrimethoxysilane (AEPTMS, technical grade), 2-cyanoethyl triethoxysilane (CETES, ≥ 97.0%), hexadecyltrimethylammonium bromide (CTAB, ≥ 99%), Brij®-56, sodium dodecyl sulfate (SDS, ≥ 98.5%), Triton® X-100, hexadecane (≥ 99%), doxorubicin hydrochloride (≥ 98%), 5-fluorouracil (≥ 99%), *cis*-diammineplatinum(II) dichloride (cisplatin, ≥ 99.9%), diphtheria toxin from *Corynebacterium diphtheriae*, cyclosporin A from *Tolypocladium inflatum* (CsA, ≥ 95%), *N*-Acetyl-L-cysteine (NAC, ≥99%), human epidermal growth factor, L-α-phosphatidylethanolamine, thymidine (≥ 99%), hypoxanthine (≥ 99%), bovine fibronectin, bovine collagen type I, gelatin, soybean trypsin inhibitor (≥ 98%), 2-mercaptoethanol (≥ 99.0%), DL-dithiothreitol (≥ 99.5%), dimethyl sulfoxide (≥ 99.9%), pH 5 citric acid buffer, ethylenediaminetetraacetic acid (EDTA, 99.995%), 4-(2-Hydroxyethyl)piperazine-1-ethanesulfonic acid (HEPES, ≥ 99.5%), ammonium phosphate dibasic (≥ 99.99%), and Sepharose® CL-4B were purchased from Sigma-Aldrich (St. Louis, MO). ABIL® EM 90 (cetyl PEG/PPG-10/1 dimethicone) was purchased from Evonik Industries (Essen, Germany). Ultra pure, EM-grade formaldehyde (16%, methanol-free) was purchased from Polysciences, Inc. (Warrington, PA). Hellmanex® II was purchased from Hellma (Müllheim, Germany).

Lipids

1,2-dioleoyl-*sn*-glycero-3-phosphocholine (DOPC), 1,2-dipalmitoyl-*sn*-glycero-3-phosphocholine (DPPC), 1,2-distearoyl-*sn*-glycero-3-phosphocholine (DSPC), 1,2-dioleoyl-3-trimethylammonium-propane (18:1 DOTAP), 1,2-dioleoyl-*sn*-glycero-3-phospho-(1'-*rac*-glycerol) (DOPG), 1,2-dioleoyl-*sn*-glycero-3-phosphoethanolamine (DOPE), 1,2-dipalmitoyl-*sn*-glycero-3-phosphoethanolamine (DPPE), 1,2-dioleoyl-*sn*-glycero-3-

phosphoethanolamine-N-[methoxy(polyethylene glycol)-2000] (18:1 PEG-2000 PE), 1,2-dipalmitoyl-*sn*-glycero-3-phosphoethanolamine-N-[methoxy(polyethylene glycol)-2000] (16:0 PEG-2000 PE), 1-Oleoyl-2-[12-[(7-nitro-2-1,3-benzoxadiazol-4-yl)amino]lauroyl]-*sn*-Glycero-3-Phosphocholine (18:1-12:0 NBD PC), 1-palmitoyl-2-{12-[(7-nitro-2-1,3-benzoxadiazol-4-yl)amino]lauroyl}-*sn*-glycero-3-phosphocholine (16:0-12:0 NBD PC), and cholesterol were purchased from Avanti Polar Lipids, Inc. (Alabaster, AL).

Cell Lines and Growth Media

Human Hep3B (HB-8064), human hepatocytes (CRL-11233), human peripheral blood mononuclear cells (CRL-9855), human umbilical cord vein endothelial cells (CRL-2873), T lymphocytes (CRL-8293), B lymphocytes (CCL-156), Eagle's Minimum Essential Medium (EMEM), Dulbecco's Modified Eagle's Medium (DMEM), Iscove's Modified Dulbecco's Medium (IMDM), RPMI 1640 medium, fetal bovine serum (FBS), and 1X trypsin-EDTA solution (0.25% trypsin with 0.53 mM EDTA) were purchased from American Type Culture Collection (ATCC; Manassas, Virginia). BEGM Bullet Kits were purchased from Lonza Group Limited (Clonetics; Walkersville, MD). DMEM without phenol red was purchased from Sigma-Aldrich (St. Louis, MO).

Fluorescent Stains and Microscopy Reagents

Hoechst 33342 (350/461), 4´,6-diamidino-2-phenylindole (DAPI, 356/451), Alexa Fluor® 405 carboxylic acid, succinimidyl ester (401/421), CellTracker™ Violet BMQC (415/516), CellTracker™ Green CMFDA (492/517), calcein (495/515), Alexa Fluor® 488 conjugate of annexin V (495/519), Alexa Fluor® 488 goat anti-mouse IgG (H+L) (495/519), Click-iT® AHA Alexa Fluor® 488 Protein Synthesis HCS Assay (495/519), LIVE⁄DEAD® Fixable Green Dead Cell Stain Kit (495/519), SYTOX® Green nucleic acid stain (504/523), MitoSOX™ Red mitochondrial superoxide indicator (510/580), Alexa Fluor® 532 carboxylic acid, succinimidyl ester (532/554), propidium iodide (535/617), pHrodo™ succinimidyl ester (558/576), CellTracker™ Red CMTPX (577/602), Texas Red® 1,2-dihexadecanoyl-*sn*-glycero-3-phosphoethanolamine (Texas Red® DHPE, 583/608), Alexa Fluor® 647 hydrazide (649/666), Alexa Fluor® 647 carboxylic acid, succinimidyl ester (650/668), Ulysis™ Alexa Fluor® 647 Nucleic Acid Labeling Kit (650/670), Alexa Fluor® 647 conjugate of

annexin V (650/665), *SlowFade*® Gold antifade reagent (with and without DAPI), Image-iT® FX signal enhancer, 1X Dulbecco's phosphate-buffered saline (D-PBS), bovine albumin fraction V solution (BSA, 7.5%), and transferrin were purchased from Invitrogen Life Sciences (Carlsbad, CA). Red Fluorescent Protein (RFP, 557/585), CaspGLOW™ Fluorescein Active Caspase-3 Staining Kit (485/535), and CaspGLOW™ Red Active Caspase-8 Staining Kit (540/570) were purchased from BioVision, Inc. (Mountain View, CA). Water soluble CdSe/ZnS quantum dots, CZWD640 (640/660), were purchased from NN-Labs (Fayetteville, AR).

Crosslinkers

1-Ethyl-3-[3-dimethylaminopropyl]carbodiimide hydrochloride (EDC), succinimidyl 4-[*N*-maleimidomethyl]cyclohexane-1-carboxylate (SMCC), *N*-[ß-Maleimidopropionic acid] hydrazide (BMPH), succinimidyl-[(*N*-maleimidopropionamido)-tetracosaethyleneglycol] ester ($SM(PEG)_{24}$), succinimidyl 6-[3´-(2-pyridyldithio)-propionamido] hexanoate (LC-SPDP), and the Sulfhydryl Addition Kit were purchased from Pierce Protein Research Products (Thermo Fisher Scientific LSR; Rockford, IL).

Silica Nanoparticles

Sub-5-nm silicon nanoparticles were purchased from Melorium Technologies, Inc. (Rochester, NY). 10-20 nm silicon oxide nanoparticles were purchased from SkySpring Nanomaterials, Inc. (Houston, TX). 30-nm, 40-nm, 50-nm, 60-nm, 70-nm, 80-nm, 90-nm, 100-nm, 150-nm, 200-nm, and 10-µm silica particles were purchased from Discovery Scientific, Inc. (Vancouver, British Columbia).

Synthetic siRNA and Peptides

Silencer select siRNAs (siRNA IDs for EGFR, VEGFR-2, and PDGFR-α are s565, s7824, and s10234, respectively) were purchased from Ambion, Inc. (Austin, TX). The double stranded-DNA oligonucleotide (5'-AAACATGTGGATTACCCATGTC-3') with 5' amino modifier C12 was purchased from Integrated DNA Technologies (IDT; Coralville, IA). 'Free' SP94 peptide (H_2N-**SFSIILTPILPL**-COOH), SP94 peptide modified with C-terminal Cys for conjugation (H_2N-**SFSIILTPILPL**GGC-COOH), and SP94 peptide used in

the Figure 4c recruitment experiments (H_2N-**SFSIILTPILPL**EEEGGC-COOH) were synthesized by New England Peptide (Gardner, MA). The H5WYG peptide (H_2N-**GLFHAIAHFIHGGWHGLIHGWYG**GGC-COOH) and nuclear localization sequence (H_2N-**NQSSNFGPMKGGNFGGRSSGPYGGGGQYFAKPRNQGGY**GGC-COOH) were synthesized by Biopeptide Co., Inc. (San Diego, CA). The emboldened portions of peptides are the original sequences; additional amino acid residues were added for conjugation or labeling purposes. All antibodies (CHALV-1, anti-Rab11a, anti-LAMP-1, anti-EGFR, anti-VEGFR-2, anti-PDGFR-α) were purchased from Abcam, Inc. (Cambridge, MA).

2. Cell Culture Conditions

Hep3B, hepatocytes, PBMCs, T-lymphocytes, and B-lymphocytes were obtained from ATCC and grown per manufacturer's instructions. Briefly, Hep3B was maintained in EMEM with 10% FBS. Hepatocytes were grown in flasks coated with BSA, fibronectin, and bovine collagen type I; the culture medium used was BEGM (gentamycin, amphotericin, and epinephrine were discarded from the BEGM Bullet kit) with 5 ng/mL epidermal growth factor, 70 ng/mL phosphatidylethanolamine, and 10% FBS. HUVECs were grown in DMEM with 20% FBS; gelatin-coated flasks were used to promote adhesion. PBMCs, T lymphocytes, and B lymphocytes were maintained in suspension flasks (Greiner Bio-One; Monroe, NC). PBMCs were grown in IMDM supplemented with 0.02 mM thymidine, 0.1 mM hypoxanthine, 0.05 mM 2-mercaptoethanol, and 10% FBS. T and B lymphocytes were grown in IMDM with 20% FBS and RPMI 1640 medium with 20% FBS, respectively. All cells were maintained at 37°C in a humidified atmosphere (air supplemented with 5% CO_2). Adherent cells were passaged with 0.05% trypsin at a sub-cultivation ratio of 1:3, while non-adherent cells were seeded at a density of 2×10^5 cells/mL and maintained at $1\text{-}5 \times 10^6$ cells/mL.

3. Synthesis and Characterization of Nanoporous Silica Particles

Synthesis of Unimodal Silica Nanoparticles

The aerosol-assisted evaporation-induced self-assembly method that we employed to prepare nanoporous silica particles with unimodal porosity has been described by Lu, *et al.*[2]. Briefly, a homogenous sol containing a silica precursor (TEOS), a structure-directing surfactant (CTAB, initially at a concentration much less than the critical micelle concentration, or CMC), and HCl dissolved in a solution of water and ethanol was aerosolized using a commercial atomizer (Model 9302A; TSI, Inc.; St Paul, MN). Nitrogen was used as the carrier gas, and all heating zones were maintained at 400°C to evaporate the solvent and increase the effective surfactant concentration. Pressure drop at the pinhole was 20 psi. Particles were collected on a Durapore membrane filter (Millipore; Billerica, MA) maintained at 80°C. A typical reaction mixture contained 55.9 mL of deionized H_2O, 43 mL of 200-proof ethanol, 1.10 mL of 1.0 N HCl, 4.0 g of CTAB, and 10.32 g of TEOS. To prepare nanoporous silica particles that dissolve more rapidly under intracellular (neutral pH, relatively high salt concentrations) conditions, various amounts of TEOS and AEPTMS, an amine-containing silane, were incorporated into the precursor sol, and the pH of the system was adjusted to 2.0 using concentrated HCl. For example, to prepare particles with 15 wt% AEPTMS, 9.36 g of TEOS and 1.33 g of AEPTMS were used.

Synthesis of Multimodal Silica Nanoparticles

The emulsion processing used to synthesize nanoporous silica particles with multimodal porosity has been described by Carroll, *et al.*[1]. Briefly, 1.82 g of CTAB (soluble in the aqueous phase) was added to 20 g of deionized water, stirred at 40°C until dissolved, and allowed to cool to 25°C. 0.57 g of 1.0 N HCl, 5.2 g of TEOS, and 0.22 g of NaCl were added to the CTAB solution, and the resulting sol was stirred for 1 hour. An oil phase composed of hexadecane with 3 wt% Abil EM 90 (a non-ionic emulsifier soluble in the oil phase) was prepared. The precursor sol was combined with the oil phase (1:3 volumetric ratio of sol:oil) in a 1000-mL round-bottom flask, stirred vigorously for 2 minutes to promote formation of a water-in-oil emulsion, affixed to a rotary evaporator (R-205; Buchi Laboratory Equipment; Switzerland), and placed in an 80°C water bath for 30 minutes. The mixture was then boiled under a reduced pressure of 120 mbar (35 rpm for 3 hours) to remove the solvent. Particles were the centrifuged (Model Centra MP4R; International Equipment Company; Chattanooga, TN) at 3000 rpm for 20 minutes, and the supernatant was decanted. Finally, the particles were calcined at 500°C

for 5 hours to remove surfactants and other excess organic matter. As described by Carroll, *et al*., solvent extraction enriches the aqueous phase in CTAB (> CMC), and the resulting micelles template 6-12 nm pores upon condensation of silica particles (in the aqueous phase). Additionally, adsorption of two surfactants (CTAB and Abil EM 90) at the water-oil interface synergistically decreases the interfacial tension, which results in the spontaneous formation of 20-30 nm microemulsion droplets that template large, surface-accessible pores.

Characterization of Silica Nanoparticles

Dynamic light scattering of nanoporous silica particles was performed using a Zetasizer Nano (Malvern; Worcestershire, United Kingdom). Samples were prepared by diluting 48 µL of silica particles (25 mg/mL) in 2.4 ml of 1X D-PBS. Solutions were transferred to 1 mL polystyrene cuvettes (Sarstedt; Nümbrecht, Germany) for analysis. Nitrogen sorption was performed using an ASAP 2020 Surface Area and Porosity Analyzer (Micromeritics Instrument Corporation; Norcross, GA). Zeta potential measurements were made using a Zetasizer Nano (Malvern; Worcestershire, United Kingdom). In a typical experiment, silica particles, liposomes, or protocells were diluted 1:50 in a simulated body fluid (pH 7.4) or citric acid buffer (pH 5.0), both of which were adjusted to contain 150 mM NaCl, and transferred to 1-mL folded capillary cells (Malvern; Worcestershire, United Kingdom) for analysis. See Supplementary Figure 1 for DLS and nitrogen sorption data and Supplementary Figure 12 for zeta potential values of silica nanoparticles, liposomes, and protocells.

4. Synthesis, Loading, and Surface Functionalization of Protocells

Liposome Fusion to Nanoporous Silica Particles

[The procedure used to synthesize protocells has been described by Liu, *et al*.[25-27] and will be mentioned only briefly. Lipids were ordered from Avanti Polar Lipids pre-dissolved in chloroform and stored at -20°C. Immediately prior to protocell synthesis, 2.5 mg of lipid was dried under a stream of nitrogen and placed in a vacuum oven (Model 1450M, VWR International, West Chester, PA) overnight to remove residual solvent. Lipids were re-hydrated in 0.5X D-PBS at a concentration of 2.5 mg/mL and were passed through a 100-nm

filter at least 10 times using a Mini-Extruder set (Avanti Polar Lipids, Inc.; Alabaster, AL). DPPC and DSPC were dissolved in 0.5X D-PBS pre-warmed to their respective transition temperatures (41°C and 55°C) and maintained at 60°C during the extrusion process. Resulting liposomes (~120-nm in diameter) were stored at 4°C for no more than one week. Nanoporous silica cores were dissolved in 0.5X D-PBS (25 mg/mL) and exposed to an excess of liposomes (1:2 - 1:4 volumetric ratio of lipid:silica) for 30-90 minutes at room temperature. Protocells were stored in the presence of excess lipid for up to 3 months at 4°C. To remove excess lipid, protocells were centrifuged at 10,000 rpm for 5 minutes, washed twice, and re-suspended in 0.5X D-PBS.

Optimization of the Supported Lipid Bilayer Composition

The composition of the SLB was optimized to minimize non-specific binding and toxicity to control cells; see Supplementary Figure 4 for structures of the various lipids that were used. The protocells used in all surface binding, internalization, and delivery experiments had SLBs composed of DOPC (or DPPC) with 5 wt% DOPE (or DPPE), 30 wt% cholesterol, and 5 wt% 18:1 (or 16:0) PEG-2000 PE. If necessary, fluorescent lipids (18:1-12:0 NBD-PC, 16:0-12:0 NBD-PC, or Texas Red® DHPE) were incorporated into the SLB at 1-5 wt%. Lipids were lyophilized together prior to rehydration and extrusion; for example 75 µL of DOPC (25 mg/mL), 5 µL of DOPE (25 mg/mL), 10 µL of cholesterol (75 mg/mL), 5 µL of 18:1 PEG-2000 PE (25 mg/mL), and 5 µL of 18:1-12:0 NBD-PC (5 mg/mL) were combined and dried to form liposomes composed of DOPC with 5 wt% DOPE, 30 wt% cholesterol, 5 wt% PEG-2000, and 1 wt% NBD-PC.

Modification of the Supported Lipid Bilayer with Various Types of Targeting Ligands

The specific affinity of protocells for HCC was optimized by conjugating various types of targeting ligands in various densities to the SLB. The SP94 and H5WYG peptides (synthesized with C-terminal cysteine residues) were conjugated to primary amines present in the head groups of PE via the heterobifunctional crosslinker, NHS-$(PEG)_n$-maleimide, which is reactive toward sulfhydryl and amine moieties and possesses a PEG spacer arm, the length of which can be altered to optimize specific affinity. $SM(PEG)_{24}$ was used in most studies (spacer arm = 9.52 nm). Amine moieties present in transferrin, anti-EGFR, and CHALV-1 were converted to

free sulfhydryls using the Sulfhydryl Addition Kit (per manufacturer's instructions). Functionalized transferrin and antibodies were conjugated to PE in the SLB using $SM(PEG)_{24}$. Ligand density was controlled by both reaction stoichiometry and incubation time. For example, protocells were incubated with a 10-fold molar excess of SP94 for 2 hours at room temperature to attain a peptide density of 0.015 wt% (~6 peptides/protocell), whereas protocells were incubated with a 5000-fold molar excess of SP94 overnight at 4°C to attain a peptide density of 5.00 wt% (~2048 peptides/protocell). Average ligand density was determined by Tricine-SDS-PAGE (SP94 and H5WYG peptides) or Laemmli-SDS-PAGE (transferrin, anti-EGFR, and CHALV-1)[28]. Briefly, protocells were modified with various ligand densities using LC-SPDP (spacer arm = 1.57 nm), a heterobifunctional crosslinker that reacts with primary amine and sulfhydryl moieties and is cleavable via reduction. Protocells were exposed to 10 mM dithiothreitol (DTT) for 30 minutes and centrifuged at 10,000 rpm for 5 minutes; the resulting supernatant contained free ligands, the concentration of which was determined via SDS-PAGE by comparing the band intensity of each sample to a standard curve using Image J Image Processing and Analysis software (National Institutes of Health; Bethesda, MD). 20% gels (with 6% bis-acrylamide and 6 M urea) were used to analyze the SP94 and H5WYG peptide densities. 10% gels were employed to analyze antibody (anti-EGFR and CHALV-1) densities, while 15% gels were used to analyze the density of transferrin.

Preparation of Fluorescently-Labeled Nanoporous Cores

Nanoporous cores were fluorescently-labeled by adding 100 µL of particles (25 mg/mL) to 900 µL of 20% APTES in 0.5X D-PBS; the particles were incubated in APTES overnight at room temperature, centrifuged (10,000 rpm, 5 minutes) to remove unreacted APTES, and re-suspended in 1 mL of 0.5X D-PBS. An amine-reactive fluorophore (e.g. Alexa Fluor® 647 carboxylic acid, succinimidyl ester; 1 mg/mL in DMSO) was added (5 µL of dye per mL of particles), and the particles were kept at room temperature for 2 hours prior to being centrifuged to remove unreacted dye. Fluorescently-labeled particles were stored in 0.5 X D-PBS at 4°C.

Loading of Unimodal Cores and Liposomes with Chemotherapeutic Drugs

Prior to liposome fusion, unimodal nanoporous cores modified to contain 15 wt% AEPTMS (25 mg/mL) were soaked in doxorubicin (5 mM) or a mixture of doxorubicin, cisplatin, and 5-fluorouracil (5 mM of each drug) for 1 hour at room temperature. Excess drug was removed via centrifugation of the particles at 10,000 rpm for 5 minutes. 120-nm liposomes were loaded with DOX using an ammonium phosphate gradient-based method that has been described previously[29]. Briefly, lipid films were re-hydrated with 300 mM $(NH_4)_2HPO_4$, and the liposome solution was extruded through a 100-nm membrane at least 10 times. Liposomes were equilibrated with an isotonic buffer solution (140 mM NaCl, 10 mM HEPES, pH 7.4) via dialysis (Float-A-Lyzer G2 dialysis units, 3.5-5 kDa MWCO; Spectrum Laboratories, Inc.; Rancho Dominguez, CA) and incubated with doxorubicin HCl (1:3 drug:lipid molar ratio) overnight at 4°C. Excess DOX was removed via size-exclusion chromatography on a 0.7 cm x 10 cm Sepharose® CL-4B column. Liposomes were loaded with 5-FU or cisplatin as described previously[30-31].

Loading of Multimodal Cores with the Multicomponent Mixture, siRNA, and Diphtheria Toxin A-Chain

Multimodal nanoporous cores modified to contain 20 wt% AEPTMS (25 mg/mL) were soaked in a solution of calcein (5 mM), Alexa Fluor® 647-labeled dsDNA oligonucleotides (100 μM), RFP (100 μM), and CdSe/ZnS quantum dots (10 μM) for 4 hours; the concentration of each cargo was varied in order to attain the optimal fluorescence intensity for hyperspectral imaging. Calcein was modified with the NLS (synthesized with a C-terminal cysteine residue) by dissolving 1 mg each of calcein and the NLS in 850 μL of 1X D-PBS; 100 μL of EDC (10 mg/mL in deionized water) and 50 μL of BMPH (10 mg/mL in DMSO) were added, and the mixture was incubated for 2 hours at room temperature. Excess calcein was removed via dialysis (Slide-A-Lyzer mini dialysis units, 2 kDa MWCO; Thermo Fisher Scientific LSR; Rockford, IL). The dsDNA oligonucleotide was labeled using the Ulysis™ Alexa Fluor® 647 Nucleic Acid Labeling Kit (per manufacturer's instructions) and modified with the NLS by combining 50 μL of dsDNA (2 mM in deionized water) with 50 μL of the NLS (1 mM in DMSO) and 10 μL of SMCC (10 mg/mL in DMSO); the mixture was incubated at room temperature for 2 hours, and excess NLS was removed via dialysis (Slide-A-Lyzer mini dialysis units, 7 kDa MWCO; Thermo Fisher Scientific LSR; Rockford, IL). For the delivery experiments described in Supplementary Figures 13-16,

multimodal nanoporous cores modified with 20 wt% AEPTMS (25 mg/mL) were soaked in siRNA (100 µM) or diphtheria toxin A-chain (100 µM) for 2 hours at 4°C. Unencapsulated cargo was removed via centrifugation at 10,000 rpm for 5 minutes, and liposomes were immediately fused to cargo-loaded cores.

5. Temperature-Dependent Fluorescence Recovery after Photobleaching (FRAP) Experiments

To obtain data depicted in Figure 2b (and Supplementary Figure 3b), DPPC (or DOPC) liposomes containing 5 wt% 16:0-12:0 NBD-PC (or 18:1-12:0 NBD-PC) were synthesized as described above and fused to porous (formed via aerosol-assisted EISA) and non-porous (purchased from Discovery Scientific, Inc.) silica particles approximately 10-µm in diameter. The resulting protocells were washed extensively (8-10 times) in 0.5X D-PBS and used immediately. Protocells (25 mg/mL) were diluted 1:1000 in 0.5X D-PBS and allowed to settle in a 35-mm glass-bottom dish (No. 1.5; MatTek Corporation; Ashland, MA). The glass-bottom dish was placed in a PeCon GmbH heated stage (Erbach, Germany) mounted to a Zeiss LSM510 Meta confocal fluorescence microscope (see below for details). A 63X, 1.4-NA objective was used to focus on green-fluorescent DPPC or DOPC bilayers. Approximately ¼ of the bilayer was photobleached (6-µm circular bleach region) at 25°C, and the temperature- or time-dependent fluorescence recovery was monitored using LSM510 software. Two scans were taken before bleaching to measure the initial fluorescence intensity of the bilayer. The 6-µm region was exposed to the 488-nm Argon laser (100% transmission, 60% output) for 8 iterations in order to reduce the fluorescence intensity to ~20% of its initial value. Recovery was monitored for 250 seconds in 1-second intervals; the 488-nm laser power was reduced to 2% transmission during recovery to minimize further photobleaching. The fluorescence intensity in the photobleached region (region of interest 1) was divided by the fluorescence intensity in a non-photobleached region (region of interest 2) to account for photobleaching that occurred during recovery. The resulting normalized recovery profiles were plotted against temperature based on the ramp rate of the heated stage (~ 0.1°C per second).

6. Determination of Dissociation Constants and Other Flow Cytometry Experiments

Construction of Saturation Binding Curves and Determination of Dissociation Constants

The following procedure was used to calculate dissociation constants (see Figures 4a and 4b, as well as Supplementary Figures 6-8). Adherent and non-adherent cells were grown in suspension flasks (Greiner Bio-One; Monroe, NC) to 70-80% confluence or 1 x 10^7 cells/mL, respectively. Adherent cells were harvested via gentle shaking in 5 mM EDTA (diluted in D-PBS) for 30 minutes at 37°C. Cells were counted (Cellometer® automated cell counter; Nexcelom Biosciences; Lawrence, MA), and 1 x 10^6 cells/mL were placed in siliconized tubes (2.0 mL G-tubes; Bio Plas, Inc.; San Rafael, CA), centrifuged at 4000 rpm for 2 minutes, washed twice with 1X D-PBS, and re-suspended in complete growth medium. Increasing concentrations (0.01 nM to 10,000 nM, depending on the experiment) of protocells or liposomes (labeled with 1 wt% Texas Red® DHPE) were incubated with 1 x 10^6 cells/mL for 1 hour at 4°C under gentle agitation. One hour is a sufficient period of time for the number of surface-bound particles to reach equilibrium; SP94-modified protocells and liposomes exhibit saturable binding. Cells were washed four times with 1X D-PBS, and re-suspended in 1 mL of serum-free DMEM without phenol red. Cell samples were analyzed with a FACSCalibur flow cytometer (Becton Dickinson; Franklin Lakes, NJ) equipped with BD CellQuest™ software, version 5.2.1. Samples were acquired with the fsc channel in linear mode and all other channels in log mode. Events were triggered based upon forward light scatter, and a gate was placed on the forward scatter-side scatter plot that excluded cellular debris. Samples were excited using the 488-nm laser source, and emission intensity was collected in the FL2 channel (585/42 filter/bandpass). Mean fluorescence intensity was determined using FlowJo Software, version 6.4 (Tree Star, Inc.; Ashland, OR). GraphPad Prism (GraphPad Software, Inc.; La Jolla, CA) was employed to generate saturation binding curves, subtract the contribution of non-specific binding (i.e. binding of unmodified protocells or liposomes) from total binding (i.e. binding of SP94-targeted protocells or liposomes), and calculate K_d values. All graphs were generated using Sigma Plot, version 11.0 (Systat Software, Inc.; San Jose, CA).

Determination of the Average Number of Protocells and Liposomes Internalized by Hep3B and Hepatocytes

The average number of SP94-targeted protocells or liposomes internalized by each Hep3B or hepatocyte cell (see Supplementary Table I) was determined using the following procedure. DOPC and DPPC protocells and liposomes (modified with 5 wt% DOPE or DPPE, 30 wt% cholesterol, 5 wt% PEG-2000, and 0.015 wt% SP94) were labeled with 1 wt% NBD-PC. DOPE or DPPE moieties were labeled with pHrodo^{TM} succinimidyl ester (per manufacturer's instructions) after conjugation of the SP94 peptide; pHrodo^{TM} SE becomes more fluorescent upon acidification of its environment, i.e. during endocytosis. 1 x 10^6 cells/mL were exposed to increasing concentrations of particles (1 x 10^6 to 1 x 10^{10}) for 1 hour at 4°C, washed, and re-suspended in cold DMEM without phenol red. Samples were analyzed using a FACSCalibur flow cytometer and gated as described above. NBD-PC was excited with the 488-nm laser, and emission intensity was collected in the FL1 channel (530/30). Mean fluorescence intensity was determined using FlowJo Software, and mean fluorescence intensity versus particle concentration data were transformed into Scatchard plots using GraphPad Prism. The average number of particles that bind to each Hep3B cell under saturating conditions was calculated from B_{max} values. Samples were then incubated at 37°C for 4 hours to enable endocytosis of surface-bound particles, and the mean fluorescence intensities of NBD-PC and pHrodo^{TM} SE were measured (the 488-nm laser was used as the excitation source, and emission intensity was collected in the FL2 channel) and plotted against particle concentration. B_{max} values were determined from Scatchard plots and used to calculate the average number of SP94-targeted protocells and liposomes endocytosed by each Hep3B or hepatocyte cell within an hour. This analysis was repeated for DOPC and DPPC protocells (modified with 30 wt% cholesterol, 5 wt% PEG-2000, and 0.015 wt% SP94) formed on 4, 10, 30, 40, 50, 60, 70, 80, 90, 100, 150, and 200-nm silica cores (see Supplementary Figure 9).

7. Preparation of Confocal Fluorescence Microscopy Samples

Peptide Recruitment Experiments

To obtain the data depicted in Figure 4c, planar SLBs were formed by fusing 50-nm liposomes to porous silica thin films coated on coverslips (25-mm, No. 1.5; Electron Microscopy Sciences; Hatfield, PA). Coverslips were pre-washed via sonication in 2% Hellmanex® II (3 x 5 minutes at 50°C) and spin-coated (2000 rpm) with a sol containing 2.4 mL of TEOS, 0.65 g of CETES, 0.56 g of Brij®-56, 15.5 mL of absolute ethanol, and 1.25 mL of 0.07 N HCl; the sol was sonicated to dissolve the Brij®-56 and aged for 2 hours. Upon calcination at 400°C for 1 hour, the resulting cubic thin film (300-400 nm thick) was well-ordered with pores oriented perpendicular to the coverslip. Liposomes were composed of either DOPC with 5 wt% DOPE and 2 wt% 18:0-12:0 NBD-PC or DPPC with 5 wt% DPPE and 2 wt% 16:0-12:0 NBD-PC and were prepared as described above. Liposomes were diluted to 100 μM with 5 mM $CaCl_2$ in 0.5X D-PBS, thin films were exposed to the diluted liposome suspension for 30 minutes at room temperature, and the resulting planar bilayers were washed extensively with 0.5X D-PBS. Planar bilayers were modified with a low density (0.015 wt%) of Alexa Fluor® 647-labeled SP94 peptides using the heterobifunctional crosslinker, $SM(PEG)_{24}$ (see above for more details). SP94 was synthesized with three glutamic acid residues near the C-terminus and was fluorescently labeled via incubation with an excess of EDC and Alexa Fluor® 647 hydrazide; unreacted dye was removed via dialysis (Float-A-Lyzer G2 dialysis units, 500 Da MWCO; Spectrum Laboratories, Inc.; Rancho Dominguez, CA). Hep3B was grown in suspension flasks to 70-80% confluence, harvested (5 mM EDTA, 30 minutes), centrifuged at 4000 rpm for 2 minutes, and re-suspended in complete growth medium. Immediately before the experiment, cells were stained with Hoechst 33342 and CellTracker™ Red CMTPX (per manufacturer's instructions), washed, and suspended in 1X D-PBS. Fluorescently-labeled Hep3B cells were added to the planar SLBs at 4°C or 37°C, and the time-dependent fluorescence intensity of the peptide was monitored at the cell-bilayer interface using a Zeiss LSM510 Meta confocal fluorescence microscope (see below).

Internalization of SP94-Targeted Protocells and Delivery of Multicomponent Cargos

To obtain results depicted in Figure 4d, Figure 4e, Figure 5 b-d, and Supplementary Figures 10-11, cells were grown in culture flasks to 70-80% confluence, harvested (0.05% trypsin, 10 minutes), centrifuged at 4000 rpm for 2 minutes, and re-suspended in complete growth medium. $1 \times 10^4 - 1 \times 10^6$ cells/mL were seeded on sterile

coverslips (25-mm, No. 1.5) coated with 0.01% poly-L-lysine (150-300 kDa) and allowed to adhere for 4-24 hours at 37°C. Cells shown in Figures 4d and 4e were exposed to a saturating concentration (~1000-fold excess) of SP94-targeted DOPC protocells with Alexa Fluor® 647-labeled cores and Texas Red®-labeled SLBs for 1 hour at 37°C, washed three times with D-PBS, stained with CellTracker™ Green CMFDA (per manufacturer's instructions), washed twice with 1X D-PBS, fixed with 3.7% formaldehyde for 10 minutes at room temperature, and mounted on 25 x 77 mm slides (VWR International, LLC.; West Chester, PA) using *SlowFade*® Gold antifade reagent with DAPI. Cells shown in Supplementary Figure 10 and 11 were exposed to a saturating concentration of DOPC protocells modified with either 0.015 wt% SP94 or with 0.015 wt% SP94 and 0.500 wt% H5WYG for 12 hours at 37°C; Alexa Fluor® 647-labeled unimodal cores were loaded with doxorubicin prior to liposome fusion, and cells were washed, fixed, and mounted as described above. Cells shown in Figure 5 were exposed to SP94-targeted DOPC protocells (Alexa Fluor® 532-labeled cores and Texas Red®-labeled SLBs) loaded with calcein, the Alexa Fluor® 647-labeled dsDNA oligonucleotide, RFP, and CdSe/ZnS quantum dots for 1 hour at 37°C. Cells were then washed three times with 1X D-PBS and placed in complete growth medium for various periods of time (e.g. 1-2 hours for endosomal localization, 2-6 hours for cytosolic localization, and 6-24 hours for nuclear localization). Cells were stained with CellTracker™ Violet BMQC and Hoechst 33342 (per manufacturer's instructions), washed twice with 1X D-PBS, fixed with 3.7% formaldehyde for 10 minutes at room temperature, and mounted using *SlowFade*® Gold antifade reagent.

Co-Localization between Protocells and Lysosomes

Cells shown in Supplementary Figure 10 were exposed to 1 x 10^9 protocells with Texas Red®-labeled SLBs for 1 hour at 37°C, washed 3 times with D-PBS, fixed with 3.7% formaldehyde (15 minutes at room temperature), permeabilized with 0.2% Triton X-100 (5 minutes at room temperature), and exposed to Image-iT® FX signal enhancer (30 minutes at room temperature); primary mouse mAbs (anti-LAMP-1 or anti-Rab11a) were incubated with the samples at a 1:500 dilution (1% BSA in D-PBS) for 1 hour at 37°C, while secondary antibodies (Alexa Fluor® 488 or 647 goat anti-mouse IgG) were incubated with the samples at a 1:250 dilution (1% BSA in D-PBS) for 90 minutes at 37°C. Samples were washed three times in 1X D-PBS between each step

and mounted with *SlowFade*® Gold containing DAPI. SlideBook software (Intelligent Imaging Innovations, Inc.; Philadelphia, PA) was used to calculate Pearson's correlation coefficients for co-localization between Texas Red®-labeled protocells and Alexa Fluor® 488-labeled LAMP-1 or Alexa Fluor® 647-labeled Rab11a.

All images were collected using a Zeiss LSM510 Meta confocal fluorescence microscope (see below for details), operated in either channel mode (3 and 4-color images) or spectral mode (8-color images).

8. Delivery of Chemotherapeutic Drugs and Drug Cocktails

Determination of Absolute and Effective Cargo Capacities

The absolute capacity of protocells and liposomes for DOX (see Figure 6a, left axis) was determined by incubating 1 x 10^{10} DOX-loaded protocells in 1 wt% SDS (dissolved in D-PBS) for 24 hours, centrifuging the solutions to remove protocell cores and other debris, and measuring the emission intensity of DOX (470/585) in the supernatant using a fluorescence microplate reader (FLx800 Fluorescence Microplate Reader; BioTex; Winooski, VT); the concentration of encapsulated DOX was calculated from a standard curve. Effective DOX capacity was determined by incubating 1 x 10^{10} SP94-targeted, DOX-loaded protocells or liposomes with 1 x 10^{6} Hep3B cells for 1 hour at 4°C. Cells were then washed 3 times with D-PBS to remove unbound particles and re-suspended in pre-warmed complete growth medium for 0, 2, 4, 8, 12, 24, 36, 48, 72, 96, and 120 hours. The time-dependent, cell-associated fluorescence intensity of DOX was measured using a FACSCalibur flow cytometer; DOX was excited with the 488-nm laser, and emission was collected in the FL2 channel. The initial mean fluorescence intensity (MFI), which corresponds to the number of DOX-loaded particles that bind to Hep3B under saturating conditions, decreased as DOX was released from protocells and liposomes in a form capable of intercalating nuclear DNA[32]. Effective capacity was calculated using the following equation: concentration of DOX (nM) encapsulated within 10^{10} particles that is released in a 'bioavailable' form = [absolute capacity (nM)]*[1-(minimum MFI/maximum MFI)]; the minimal MFI value was typically reached within 24-48 hours.

Determination of Doxorubicin Release Rates

To determine the rate of DOX release from DOPC protocells, DOPC liposomes, DSPC liposomes, and nanoporous silica cores under neutral and acidic pH conditions (see Figures 6b and 6c, respectively, as well as Supplementary Fig. 2b), 1 x 10^{10} DOX-loaded particles were suspended in 1 mL of a simulated body fluid (EMEM with 150 mM NaCl and 10% serum, pH 7.4) or citric acid buffer (pH 5.0) and maintained at 37°C for various periods of time (0, 1, 4, 8, 12, 24, 48, and 72 hours, as well as 5, 7, 10, 14, and 21 days). Particles were removed via centrifugation (5 minutes at 5,000 x g for protocells and 30 minutes at 15,000 x g for liposomes; Microfuge® 16 Centrifuge; Beckman-Coulter; Brea, CA), and the fluorescence intensity of the supernatant was measured using a microplate reader. The concentration of released DOX was calculated from a standard curve and was expressed as a percentage of the DOX that was initially encapsulated within 10^{10} particles.

Determination of LC_{90} and LC_{50} Values

The concentration of DOX necessary to kill 90% of Hep3B with induced MDR (LC_{90}) was determined by exposing 1 x 10^6 cells/mL to increasing concentrations of DOX (either in a free form or encapsulated within protocells or liposomes) for 24 hours at 37°C. Cells were centrifuged (4000 rpm, 2 minutes) to remove excess drug and stained with SYTOX® Green nucleic acid stain and Alexa Fluor® 647-labeled annexin V. The numbers of viable (double-negative) and non-viable (single- or double-positive) cells were determined via flow cytometry (FACSCalibur); SYTOX® Green fluorescence was excited by the 488-nm laser and collected in the FL1 channel, while Alexa Fluor® 647 fluorescence was excited by the 633-nm laser and collected in the FL3 channel (670-nm long pass filter). Parental Hep3B and MDR Hep3B exposed to 1 µM of CsA for 72 hours to reverse Pgp-mediated resistance[33] were used as controls (data not shown). MDR was induced in parental Hep3B via exposure to increasing concentrations of DOX in 24-hour intervals (25 nM, 50 nM, 75 nM, 100 nM, 150 nM, 200 nM, 250 nM, 300 nM, 350 nM, 400 nM, 450 nM, 500 nM, 600 nM, 700 nM, 800 nM, 900 nM, 1 µM, 1.5 µM, 2 µM, 2.5 µM, 3 µM, 4 µM, and 5 µM), interspersed with 48-hour recovery periods during which cells

were incubated in complete growth medium without DOX[34]. The same procedure was employed to determine LC_{50} values.

Determination of Particle Concentrations Necessary to Achieve LC_{90} Values and Time-Dependent Viability

The number of SP94-targeted protocells (loaded with DOX or a combination of DOX, 5-FU, and cisplatin) and liposomes (individually loaded with DOX, 5-FU, or cisplatin) necessary to kill 90% of MDR Hep3B (see Figure 6a) was determined by incubating various concentrations of particles with 1 x 10^6 cells/mL for 24 hours at 37°C. To determine the number of MDR Hep3B and hepatocytes that remained viable after exposure to 9.6 μM or 2.4 μM of DOX (either in a free form or encapsulated within protocells or liposomes; see Figure 6d), 1 x 10^6 cells/mL were exposed to the drug for 24 hours at 37°C. Cell viability was determined using SYTOX® Green and Alexa Fluor® 647-labeled annexin V as described above.

9. Delivery of a siRNA Cocktail

To determine the concentration of siRNA necessary to silence 50% of EGFR, VEGFR-2, or PDGFR-α expression (IC_{50}, see Supplementary Figure 13a), 1 x 10^6 Hep3B cells (parental) were exposed to various concentrations of siRNA loaded in SP94-targeted DOPC protocells for 24 hours at 37°C. Cells were centrifuged (4000 rpm, 2 minutes) to remove excess particles, fixed with 3.7% formaldehyde (15 minutes at room temperature), and permeabilized with 0.2% Triton X-100 (5 minutes at room temperature); cells were exposed to a 1:500 dilution of anti-EGFR, anti-VEGFR-2, or anti-PDGFR-α (1% BSA in D-PBS) for 1 hour at 37°C and to a 1:250 dilution of the secondary antibody (Alexa Fluor® 488 goat anti-mouse IgG in 1% BSA) for 90 minutes at 37°C. Cells were washed three times and re-suspended in D-PBS for flow cytometry analysis (FACSCalibur). The mean fluorescence intensity of each sample was determined via excitation of Alexa Fluor® 488 with the 488-nm laser and detection of the resulting emission in the FL1 channel. GraphPad Prism was

employed to calculate IC_{50} values from plots of log(siRNA concentration) versus mean fluorescence intensity; the initial protein concentration was taken to be the mean fluorescence intensity of antibody-labeled cells exposed to siRNA-loaded protocells for 5 minutes.

The time-dependent decrease in EGFR, VEGFR-2, and PDGFR-α expression (see Supplementary Figures 13b and 13c) was determined by exposing 1 x 10^6 cells (parental Hep3B and hepatocytes) to SP94-targeted protocells loaded with 10 nM of siRNA for 4, 8, 12, 24, 36, 48 72, 96, and 120 hours at 37°C. Resulting protein levels were determined via immunofluorescence as described above.

Cells depicted in Supplementary Figures 13d and 11e were exposed to a saturating concentration of SP94-targeted DOPC protocells (with Alexa Fluor® 647-labeled cores) loaded with 10 nM of the siRNA cocktail for either 1 hour or 72 hours at 37°C. Cells were washed 3 times with D-PBS, fixed with 3.7% formaldehyde (15 minutes at room temperature), permeabilized with 0.2% Triton X-100 (5 minutes at room temperature), and blocked with Image-iT® FX signal enhancer (30 minutes, room temperature). Cells were then exposed to primary antibodies (anti-EGFR, anti-VEGFR-2, or anti-PDGFR-α mouse mAbs; diluted 1:500 in 1% BSA) overnight at 4°C, washed 3 times in D-PBS, exposed to the secondary antibody (Alexa Fluor® 488 goat anti-mouse IgG) for 90 minutes at 37°C, and mounted with *SlowFade*® Gold containing DAPI.

The time-dependent viability of Hep3B and hepatocytes (see Supplementary Figure 14a) was determined by exposing 1 x 10^6 cells to SP94-targeted protocells loaded with 10 nM of the siRNA cocktail for various periods of time (same as above) at 37°C. Cells were centrifuged (4000 rpm, 2 minutes) to remove excess protocells and stained with Alexa Fluor 488®-labeled annexin V and propidium iodide. The number of viable (double-negative) and non-viable (single- or double-positive) cells was determined via flow cytometry (FACSCalibur).

Cells shown in Supplementary Figures 14b and 14c were exposed to SP94-targeted protocells (with Alexa Fluor® 647-labeled cores) loaded with 10 nM of the siRNA cocktail for 4 hours, 24, hours, 48 hours, 72 hours, or 168 hours. Cells were then washed 3 times with D-PBS and stained with Alexa Fluor® 488-labeled annexin

V and propidium iodide (per manufacturer's instructions), washed, fixed (3.7% formaldehyde for 10 minutes at room temperature), and mounted with *SlowFade*® Gold containing DAPI.

10. Delivery of Diphtheria Toxin A-Chain

The IC_{50} value of SP94-targeted DOPC protocells loaded with diphtheria toxin A-chain (see Supplementary Figure 15a) was determined by incubating 1 x 10^6 Hep3B cells with various concentrations of protocell-encapsulated toxin for 24 hours at 37°C. The resultant decrease in nascent protein synthesis was detected using the Click-iT® AHA Alexa Fluor® 488 Protein Synthesis HCS Assay (per manufacturer's instructions) and quantified via flow cytometry (FACSCalibur). The mean fluorescence intensity of each sample was plotted against log(toxin concentration), and the IC_{50} value was determined using GraphPad Prism.

The time-dependent decline in nascent protein synthesis (see Supplementary Figure 15b) was measured by exposing 1 x 10^6 Hep3B cells to SP94-targeted protocells loaded with 100 nM of diphtheria toxin A-chain for 4, 8, 12, 24, 36, 48 72, 96, and 120 hours at 37°C; nascent protein synthesis was assayed for as described above.

Cells shown in Supplementary Figure 15c were exposed to a saturating concentration of SP94-targeted DOPC protocells (with Alexa Fluor® 647-labeled cores) loaded with 100 nM of diphtheria toxin A-chain for 12 or 72 hours at 37°C. Newly synthesized proteins were labeled using the Click-iT® AHA Alexa Fluor® 488 Protein Synthesis HCS Assay (per manufacturer's instructions). Cells were then mounted using *SlowFade*® Gold containing DAPI.

The time-dependent activation of caspase-3 and caspase-8 (see Supplementary Figure 16a) was determined by exposing 1 x 10^6 cells (Hep3B and hepatocytes) to SP94-targeted protocells loaded with 100 nM of diphtheria toxin A-chain for various periods of time at 37°C. The degree of caspase activation was quantified using the CaspGLOW™ Fluorescein Active Caspase-3 and CaspGLOW™ Red Active Caspase-8 Staining Kits;

flow cytometry (FACSCalibur) was employed to determine the number of cells expressing green fluorescence (FL1) and/or red fluorescence (FL2) at levels 100-times higher than that of the background (viable Hep3B cells). Apoptotic cells were defined as those positive for caspase-8, caspase-3, or caspase-8 and caspase-3 activation.

Cells shown in Supplementary Figures 16b and 16c were exposed to SP94-targeted DOPC protocells (with Alexa Fluor® 647-labeled cores) loaded with diphtheria toxin A-chain for various periods of time. Active caspase-3 and active caspase-8 were labeled using the CaspGLOW™ Fluorescein Active Caspase-3 and CaspGLOW™ Red Active Caspase-8 Staining Kits (respectively). Cells were then washed 3 times in D-PBS, fixed (3.7% formaldehyde for 10 minutes at room temperature), and mounting using *SlowFade*® Gold with DAPI.

11. Confocal Fluorescence Microscopy Equipment and Settings

Three- and four-color images were acquired using a Zeiss LSM510 META (Carl Zeiss MicroImaging, Inc.; Thornwood, NY) operated in Channel mode of the LSM510 software; a 63X, 1.4-NA oil immersion objective was employed in all imaging. Typical laser power settings were: 30% transmission for the 405-nm diode laser, 5% transmission (60% output) for the 488-nm Argon laser, 100% transmission for the 543-nm HeNe laser, and 85% transmission for the 633-nm HeNe laser. Gain and offset were adjusted for each channel to avoid saturation and were typically maintained at 500-700 and -0.1, respectively. 8-bit z-stacks with 1024 x 1024 resolution were acquired with a 0.7 to 0.9-µm optical slice. LSM510 software was used to overlay channels and to create 3D projections of z-stack images. Images in Figures 4c (insets), 4d, and 4e, as well as in Supplementary Figures 10-11 and 13-16 are collapsed projections.

Eight-color images (see Figures 5b-5d) were acquired using the Zeiss LSM510 META operated in Lambda mode of the LSM510 software; a 63X, 1.4-NA objective was used. Spectral information was acquired over the entire range of the system (411.3-nm to 753.7-nm with a 10.7-nm step) and collected across the 32 PMTs. Laser power and gain were adjusted to avoid saturating the brightest components of the sample. The

following settings were used to acquire 8-bit, 1024 x 1024 z-stacks: 14% transmission for the 405-nm diode laser, 3% transmission (60% output) for the 488-nm Argon laser, 3% transmission for the 543-nm HeNe laser, and 3% transmission for the 633-nm HeNe laser; the gain was 850, the offset was -0.15, the optical slice was 0.40 µm, and the frame size was 140-µm x 160-µm. Control spectra used for unmixing were acquired using singly-labeled control samples. Images were unmixed using the advanced linear unmixing algorithm of the LSM510 software. The brightness and contrast of all channels in the unmixed images were adjusted equally (using the LSM510 software) to balance the intensity between channels. Images in Figures 5b-5d are collapsed projections.

Supplementary References

1 Carroll, N. J., Pylypenko, S., Atanassov, P. B. & Petsev, D. N. Microparticles with Bimodal Nanoporosity Derived by Microemulsion Templating. *Langmuir*, doi:10.1021/la900988j (2009).

2 Lu, Y. F. *et al.* Aerosol-assisted self-assembly of mesostructured spherical nanoparticles. *Nature* **398**, 223-226 (1999).

3 Iler, R. K. *The Chemistry of SIlica: Solubility, Polymerization, Colloid and Surface Properties, and Biochemistry*. (John Wiley and Sons, 1979).

4 Doshi, D. A. *et al.* Neutron Reflectivity Study of Lipid Membranes Assembled on Ordered Nanocomposite and Nanoporous Silica Thin Films. *Langmuir* **21**, 2865-2870, doi:10.1021/la0471240 (2005).

5 Bernhard, M. I. *et al.* Guinea Pig Line 10 Hepatocarcinoma Model: Characterization of Monoclonal Antibody and in Vivo Effect of Unconjugated Antibody and Antibody Conjugated to Diphtheria Toxin A Chain. *Cancer Research* **43**, 4420-4428 (1983).

6 Lo, A., Lin, C. T. & Wu, H. C. Hepatocellular carcinoma cell-specific peptide ligand for targeted drug delivery. *Molecular Cancer Therapeutics* **7**, 579-589, doi:10.1158/1535-7163.mct-07-2359 (2008).

7 Sciot, R. *et al.* Transferrin receptor expression in human hepatocellular carcinoma: an immunohistochemical study of 34 cases. *Histopathology* **12**, 53-63 (1988).

8 Kannangai, R., Sahin, F. & Torbenson, M. S. EGFR is phosphorylated at Ty845 in hepatocellular carcinoma. *Mod Pathol* **19**, 1456-1461 (2006).

9 Behr, J. P. The Proton Sponge: a Trick to Enter Cells the Viruses Did Not Exploit. *CHIMIA International Journal for Chemistry* **51**, 34-36 (1997).

10 Jiang, W., KimBetty, Y. S., Rutka, J. T. & ChanWarren, C. W. Nanoparticle-mediated cellular response is size-dependent. *Nat Nano* **3**, 145-150, (2008).

11 Zimmermann, R. *et al.* Charging and structure of zwitterionic supported bilayer lipid membranes studied by streaming current measurements, fluorescence microscopy, and attenuated total reflection Fourier transform infrared spectroscopy. *Biointerphases* **4**, 1-6 (2009).

12 Ashihara, E., Kawata, E. & Maekawa, T. Future Prospect of RNA Interference for Cancer Therapies. *Current Drug Targets* **11**, 345-360 (2010).

13 Pawitan, J. A. The possible use of RNA interference in diagnosis and treatment of various diseases. *International Journal of Clinical Practice* **63**, 1378-1385 (2009).

14 Elbashir, S. M. *et al.* Duplexes of 21-nucleotide RNAs mediate RNA interference in cultured mammalian cells. *Nature* **411**, 494-498 (2001).
15 Davis, M. E. *et al.* Evidence of RNAi in humans from systemically administered siRNA via targeted nanoparticles. *Nature* **advance online publication** (2010).
16 Oh, Y.-K. & Park, T. G. siRNA delivery systems for cancer treatment. *Advanced Drug Delivery Reviews* **61**, 850-862 (2009).
17 Sou, K., Endo, T., Takeoka, S. & Tsuchida, E. Poly(ethylene glycol)-Modification of the Phospholipid Vesicles by Using the Spontaneous Incorporation of Poly(ethylene glycol)-Lipid into the Vesicles. *Bioconjugate Chemistry* **11**, 372-379, doi:10.1021/bc990135y (2000).
18 Klein, E. *et al.* "HFP" Fluorinated Cationic Lipids for Enhanced Lipoplex Stability and Gene Delivery. *Bioconjugate Chemistry* **21**, 360-371, doi:10.1021/bc900469z (2010).
19 Mínguez, B., Tovar, V., Chiang, D., Villanueva, A. & Llovet, J. M. Pathogenesis of hepatocellular carcinoma and molecular therapies. *Current Opinion in Gastroenterology* **25**, 186-194 110.1097/MOG.1090b1013e32832962a32832961 (2009).
20 Li, S.-D., Chen, Y.-C., Hackett, M. J. & Huang, L. Tumor-targeted Delivery of siRNA by Self-assembled Nanoparticles. *Mol Ther* **16**, 163-169, (2007).
21 Landen, C. N. *et al.* Therapeutic EphA2 Gene Targeting In vivo Using Neutral Liposomal Small Interfering RNA Delivery. *Cancer Research* **65**, 6910-6918 (2005).
22 Honjo, T., Nishizuka, Y., Hayaishi, O. & Kato, I. Diphtheria Toxin-dependent Adenosine Diphosphate Ribosylation of Aminoacyl Transferase II and Inhibition of Protein Synthesis. *Journal of Biological Chemistry* **243**, 3553-3555 (1968).
23 Uchida, T., Kim, J. H., Yamaizumi, M., Miyake, Y. & Okada, Y. Reconstitution of lipid vesicles associated with HVJ (Sendai virus) spikes. Purification and some properties of vesicles containing non-toxic fragment A of diphtheria toxin. . *Journal of Cell Biology* **80**, 10-20 (1979).
24 Mizuguchi, H. *et al.* Application of fusogenic liposomes containing fragment A of diphtheria toxin to cancer therapy. *British Journal of Cancer* **73**, 472-476 (1997).
25 Liu, J. W., Jiang, X. M., Ashley, C. & Brinker, C. J. Electrostatically Mediated Liposome Fusion and Lipid Exchange with a Nanoparticle-Supported Bilayer for Control of Surface Charge, Drug Containment, and Delivery. *Journal of the American Chemical Society* **131**, 7567-+, doi:10.1021/ja902039y (2009).
26 Liu, J. W., Stace-Naughton, A. & Brinker, C. J. Silica nanoparticle supported lipid bilayers for gene delivery. *Chemical Communications*, 5100-5102, doi:10.1039/b911472f (2009).
27 Liu, J. W., Stace-Naughton, A., Jiang, X. M. & Brinker, C. J. Porous Nanoparticle Supported Lipid Bilayers (Protocells) as Delivery Vehicles. *Journal of the American Chemical Society* **131**, 1354-+, doi:10.1021/ja808018y (2009).
28 Schagger, H. Tricine-SDS-PAGE. *Nat. Protocols* **1**, 16-22 (2006).
29 Fritze, A., Hens, F., Kimpfler, A., Schubert, R. & Peschka-Süss, R. Remote loading of doxorubicin into liposomes driven by a transmembrane phosphate gradient. *Biochimica et Biophysica Acta (BBA) - Biomembranes* **1758**, 1633-1640 (2006).
30 Elorza, B., Elorza, M. A., Frutos, G. & Chantres, J. R. Characterization of 5-fluorouracil loaded liposomes prepared by reverse-phase evaporation or freezing-thawing extrusion methods: study of drug release. *Biochimica et Biophysica Acta* **1153**, 135-142 (1993).
31 Peleg-Shulman, T., Gibson, D., Cohen, R., Abra, R. & Barenholz, Y. Characterization of sterically stabilized cisplatin liposomes by nuclear magnetic resonance. *Biochimica et Biophysica Acta* **1510**, 278-291 (2001).

32 Bogush, T., Smirnova, G., Shubina, L., Syrkin, A. & Robert, J. Direct evaluation of intracellular accumulation of free and polymer-bound anthracyclines. *Cancer Chemotherapy and Pharmacology* **35**, 501-505, doi:10.1007/BF00686835 (1995).

33 Tong, A. W. *et al.* Chemosensitization of human hepatocellular carcinoma cells with cyclosporin A in post-liver transplant patient plasma. *Clin. Cancer Res.* **2**, 531-539 (1996).

34 Minko, T., Kopecková, P. & Kopecek, J. Chronic exposure to HPMA copolymer-bound adriamycin does not induce multidrug resistance in a human ovarian carcinoma cell line. *Journal of Controlled Release* **59**, 133-148 (1999).